Astron. Astrophys. 271, 601–620 (1993)

ASTRONOMY AND ASTROPHYSICS

Solar neutrinos and nuclear reactions in the solar interior

V. Castellani[1,2], S. Degl'Innocenti[3], and G. Fiorentini[3]

[1] Dipartimento di Fisica dell'Università di Pisa, Piazza Torricelli 2, I-56100 Pisa, Italy
[2] Osservatorio Astronomico di Collurania, I-64100 Teramo, Italy
[3] Dipartimento di Fisica dell'Università di Ferrara and Istituto Nazionale di Fisica Nucleare, Sezione di Ferrara, I-44100 Ferrara, Italy

Received May 13, accepted October 20, 1992

Abstract. We discuss the results of Homestake and Kamioka experiments, showing that – if the results of these experiments are taken at their face values – one way to save "conventional neutrinos" is to look for a nuclear solution decreasing both ^{7}Be and ^{8}B neutrino fluxes with respect to the predictions of the standard solar models. Recent GALLEX results appear in agreement with such a conclusion. We discuss the sensitivity of the ^{8}B and ^{7}Be neutrino fluxes to the behaviour of the low energy ^{3}He + ^{3}He and ^{3}He + ^{4}He cross sections. We derive analytically the dependence of the neutrino fluxes on the low energy nuclear cross sections. This analytical approach has been supported by numerical experiments based on a new Standard Solar Model. In the non-resonant case, reduction of the neutrino fluxes to about 1/3 of the Standard Solar Model could be obtained if the true value of $S_{34}(0)$ is three times smaller than the presently accepted extrapolated value. Alternatively, one should have $S_{33}(0)$ wrong by a factor nine. A resonance in the ^{3}He + ^{3}He channel could yield a sufficient reduction of ^{8}B neutrinos and, furthermore, a suppression of ^{7}Be neutrinos larger than that of ^{8}B neutrinos provided that $E_R \leq 21.4$ keV, an energy region so far almost unexplored experimentally. We show that future experiments in underground laboratories should be able to explore the region down to $E_R = 10$ keV with a significant sensitivity. We also compare our Standard Solar Model with the results of previous calculations.

Key words: Sun: interior – Sun: particle emission – nuclear reactions – elementary particles

1. Foreword

The status of the solar neutrino problem, with the Homestake and Kamioka experiments – (see Davis 1990; Hirata et al. 1990, 1991) – reporting a neutrino signal significantly smaller than the theoretical estimate (Bahcall 1989), seems to point towards unconventional neutrino properties, as flavour oscillations (Pontecorvo 1968; Gribov & Pontecorvo 1969; Wolfenstein 1978, 1979; Mikheyev & Smirnov 1986a–c), magnetic moment transitions (Voloshin et al. 1986a, b), neutrino decay (Bahcall et al. 1972; Berezhiani et al. 1987). However, preliminary results of the Soviet American Gallium experiment (Abazov et al. 1991) supporting this conclusion have been recently challenged by the result of GALLEX collaboration (1992), which gave no clear evidence against conventional neutrinos. In such a situation, since the solar neutrino problem is now extremely important, we believe that one has to be extremely critical and not to dismiss any possibility. Thus it appears worth to investigate the room left to possible errors in the theoretical estimate of solar neutrino fluxes.

In this respect, it is worth recalling that the values of the nuclear cross sections adopted in the calculations do not correspond to directly measured quantities. So far, they are always obtained by extrapolating experimental data which are measured at significantly higher energies than those relevant to the solar interior (see Rolfs & Rodney 1988 for a review on the argument). More in general, one has to observe that the theoretical values of the neutrino fluxes are based on stellar evolutionary codes which are rather complex from both the physical and numerical point of view. It is thus extremely desirable to investigate the model dependence of solar neutrino fluxes, looking for information which is independent, or very weakly dependent, on the details of the solar model calculations.

In this spirit, the main purpose of this paper is to examine which space is still left for a "nuclear physics solution" of the solar neutrino problem. We will try to get information directly from both Homestake and Kamioka data, without making assumptions on nuclear cross sections and by using as little as possible a Standard Solar Model (SSM). Next we shall discuss how the present situation can be clarified by experiments which are now in progress or in preparation. We refer of course to the Gallium detectors, which are now producing their first

Send offprint requests to: V. Castellani (first address above)

data, and we also consider the proposed Borexino experiment (Raghavan 1990; Arpesella et al. 1992), which can add significant information on this point. We will finally discuss the importance of the LUNA project, the proposal of a Laboratory for Underground Nuclear Astrophysics (Arpesella et al. 1991), where it is planned to extend measurements of the relevant nuclear cross sections down to significantly lower energies than in any previous experiment.

2. Plan of the paper

It is well known that the total number of emitted neutrinos is basically determined by Sun energetics only, and therefore it is independent of solar model calculations. As a matter of fact, if solar energy is produced by the burning of H into He, as long as the solar luminosity remains $\approx 4\ 10^{33}\,\mathrm{erg\,s^{-1}}$, the number of emitted neutrinos has to be $\approx 2\ 10^{38}\,\mathrm{s^{-1}}$ (see Fig. 1). In principle, it is possible to discuss other aspects of the solar neutrino problem independently of solar model calculations.

All in all, provided that neutrinos behave conventionally, the signal in a solar neutrino detector depends on just a few properties of the Sun, i.e. the integrated fluxes Φ_i corresponding to the neutrinos produced in different branches of the nuclear reactions chain. By using the results of a suitable series of experiments it should be possible, at least in principle, to extract all the Φ_i's. The true Φ_i's can be different from the calculated values of the SSM, for example because of the difference between true and estimated nuclear cross sections. However the important point is that values of Φ_i's extracted in this way have to be consistent among each others. Otherwise neutrinos are unconventional and/or experiments are wrong. The confidence level at which this consistency is established is an indication of the plausibility of an "astro-nuclear" solution, which would be completely independent of the solar model calculations.

We will show that by using the Homestake and Kamioka results it is already possible to get information which is only weakly dependent on the Standard Solar Model. Since we have just two experimental data, we can at most determine two (^{7}Be and ^{8}B) neutrino fluxes. We will show that one can extract consistent values of $\Phi(^7\mathrm{Be})$ and $\Phi(^8\mathrm{B})$, however only with a rather small probability. In other words, data indicate a solar neutrino problem, even without assuming the SSM to be correct. We will try to discuss quantitatively this point, which has already been noticed (see for example Bethe & Bahcall 1991).

As expected, it comes out that *both* the ^{7}Be and ^{8}B neutrino fluxes derived in this way are substantially smaller than those predicted by the Standard Solar Model calculations. How far this difference can be ascribed to a wrong estimate of some nuclear cross section? One can try to turn the question to the realm of nuclear astrophysics, particularly in connection with the new, low background and high sensitivity experiments which are being planned at the underground Gran Sasso laboratory (Arpesella et al. 1991). Assuming that the extrapolations used so far are wrong, there are values of the nuclear cross sections able to account for the observed deficit of both ^{7}Be and ^{8}B neutrino fluxes?

In order to reduce both $\Phi(^7\mathrm{Be})$ and $\Phi(^8\mathrm{B})$ one needs a mechanism that reduces the production of ^{7}Be nuclei in the Sun (see Fig. 2), i.e. a mechanism that alters the relative probabilities for the two reactions

$$^3\mathrm{He} + {}^3\mathrm{He} \rightarrow {}^4\mathrm{He} + 2\mathrm{p}, \tag{2.1}$$

$$^3\mathrm{He} + {}^4\mathrm{He} \rightarrow {}^7\mathrm{Be} + \gamma, \tag{2.2}$$

in the direction of reducing the occurrence of the latter.

Basically, there are two possibilities: (i) non resonant cross sections for the ^{3}He + ^{3}He and ^{3}He + ^{4}He reactions

Table 1. For the ith component of the neutrino flux we present:
(1) the predicted flux of our Standard Solar Model
(2) the error on the predicted fluxes, derived from Bahcall, Table 7.4. Errors to be taken as 1σ values (correspondingly the Bahcall estimate has been divided by a factor three)
(3) The M coefficients for the Homestake and Gallium experiments, see Eq. (3.1), from Bahcall (1989)

ith component	E_i(max) (MeV)	SSM predicted Flux ($\mathrm{cm^{-2}\,s^{-1}}$)	M_i^{H} (SNU $\mathrm{cm^2\,s}$)	M_i^{G} (SNU $\mathrm{cm^2\,s}$)
pp	0.42	$(6.1 \pm 0.04)\ 10^{10}$	0	$11.8\ 10^{-10}$
^{7}Be	0.86	$(4.6 \pm 0.23)\ 10^{9}$	$2.35\ 10^{-10}$	$7.3\ 10^{-9}$
^{13}N	1.20	$(5.4 \pm 0.9)\ 10^{8}$	$1.64\ 10^{-10}$	$0.62\ 10^{-8}$
pep	1.44	$(1.4 \pm 0.02)\ 10^{8}$	$14.3\ 10^{-10}$	$2.1\ 10^{-8}$
^{15}O	1.73	$(4.5 \pm 0.9)\ 10^{8}$	$5.8\ 10^{-10}$	$1.17\ 10^{-8}$
^{17}F	1.74	$(4.3 \pm 0.7)\ 10^{6}$	$5.8\ 10^{-10}$	$1.15\ 10^{-8}$
^{8}B	14.06	$(5.7 \pm 0.7)\ 10^{6}$	$1.10\ 10^{-6}$	$2.4\ 10^{-6}$
hep	18.77	$(7.5 \pm ...)\ 10^{3}$	$3.9\ 10^{-6}$	$0.79\ 10^{-5}$

with low energy astrophysical S-factors, S_{33} and S_{34}, significantly different from those so far extrapolated, (ii) a resonance in the $^3He+^3He$ channel at very low energy.

Concerning the first case, we will determine analytically the dependence of the ^7Be- and ^8B-neutrino fluxes on S_{33} and S_{34}, so that we will be able to explore the dependence of the Homestake and the Kamioka signals on these nuclear reactions parameters without relying on rather complex solar evolution codes. For the latter case, firstly considered in Fowler (1972), we will improve the analytical approach given by Krauss et al. (1987), producing an estimate of the resonance parameters (position and strength) which could account for both the Homestake and Kamioka data. On this basis we will comment on the possibility of detecting such a resonance in future experiments.

As already stated, our spirit is to gain physical information independently, as far as possible, of the use of complex stellar evolution codes. The best way to implement such a program is actually to have at disposal a stellar evolution code, as good as possible, and to use it as a theoretical laboratory, where different hypotheses can be tested and approximate analytical estimates can be checked. For this purpose, we have used the FRANEC stellar evolution code (see Appendix), developing our Standard Solar Model. The main results are summarized in Table 1 and Figs. 1 and 2. A comparison with codes and models of other groups will be given in the Appendix.

The next section will be devoted to the information on the neutrino fluxes which can be obtained independently, or almost independently, of stellar evolution codes. In Sect. 4 we will explore the dependence of the production of ^7Be nuclei as a function of the cross sections for $^3He+^3He$ and $^3He+^4He$ reactions. The general results will then be specialized to the case of non resonant cross section and the possibility of a resonance in the $^3He+^3He$ channel will be also discussed. The main conclusions of the paper are summarized in the final section. In the Appendix, our stellar evolution code and our Standard Solar Model are presented and briefly compared with the work of other groups.

3. The solar neutrino problem (almost) without the Standard Solar Model

3.1. Kamioka and Homestake

As mentioned above, let us try to derive from Kamioka and Homestake data information, the neutrino fluxes,

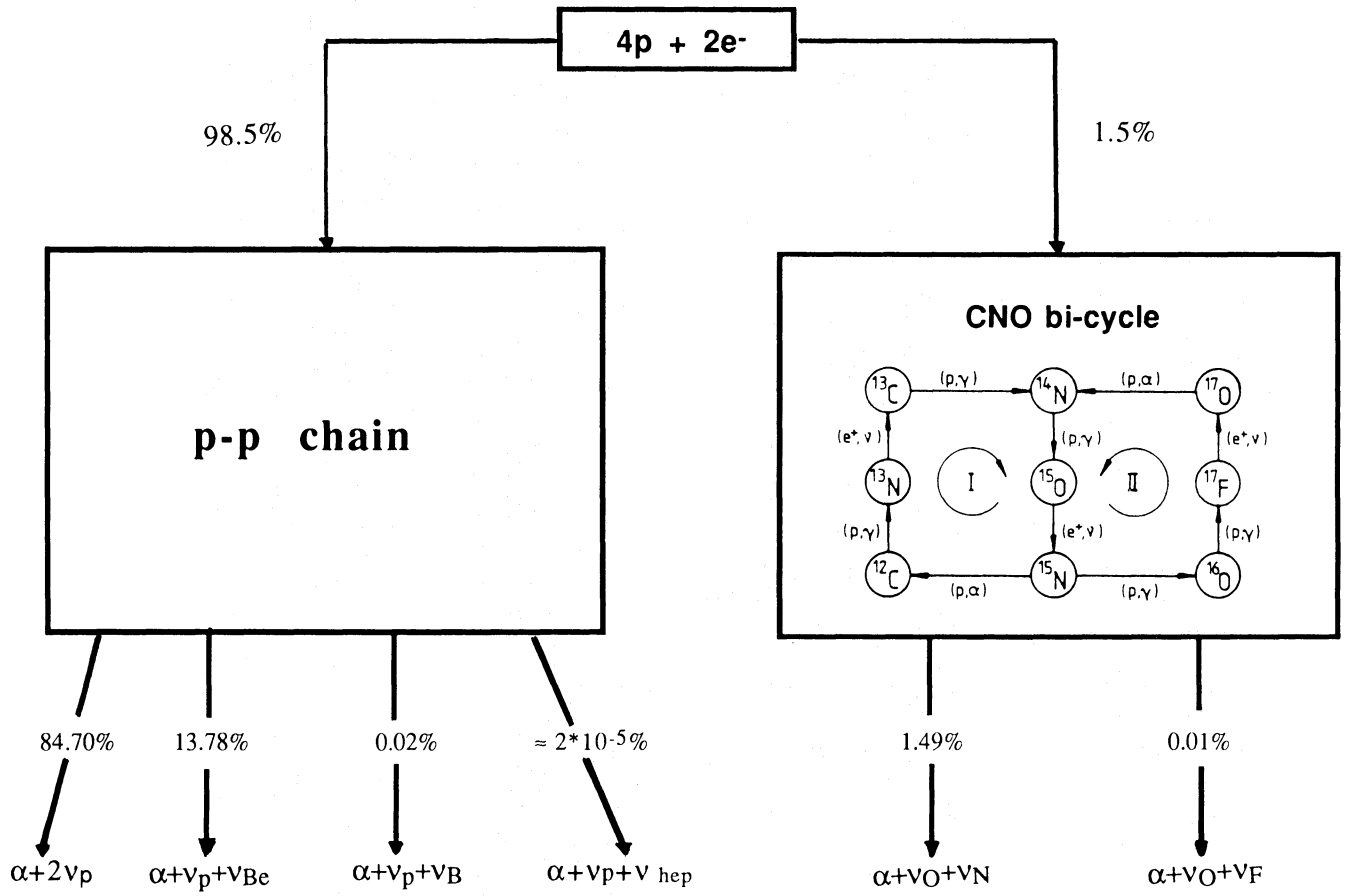

Fig. 1. The terminations of hydrogen burning reactions in the Sun. The probabilities of the different terminations correspond to the Standard Solar Model developed by using the FRANEC code. ν_p is a pp or pep neutrino (the relative probabilities being 99.77% and 0.23% respectively), ν_{Be} is a neutrino from electron capture in ^7Be, and so on

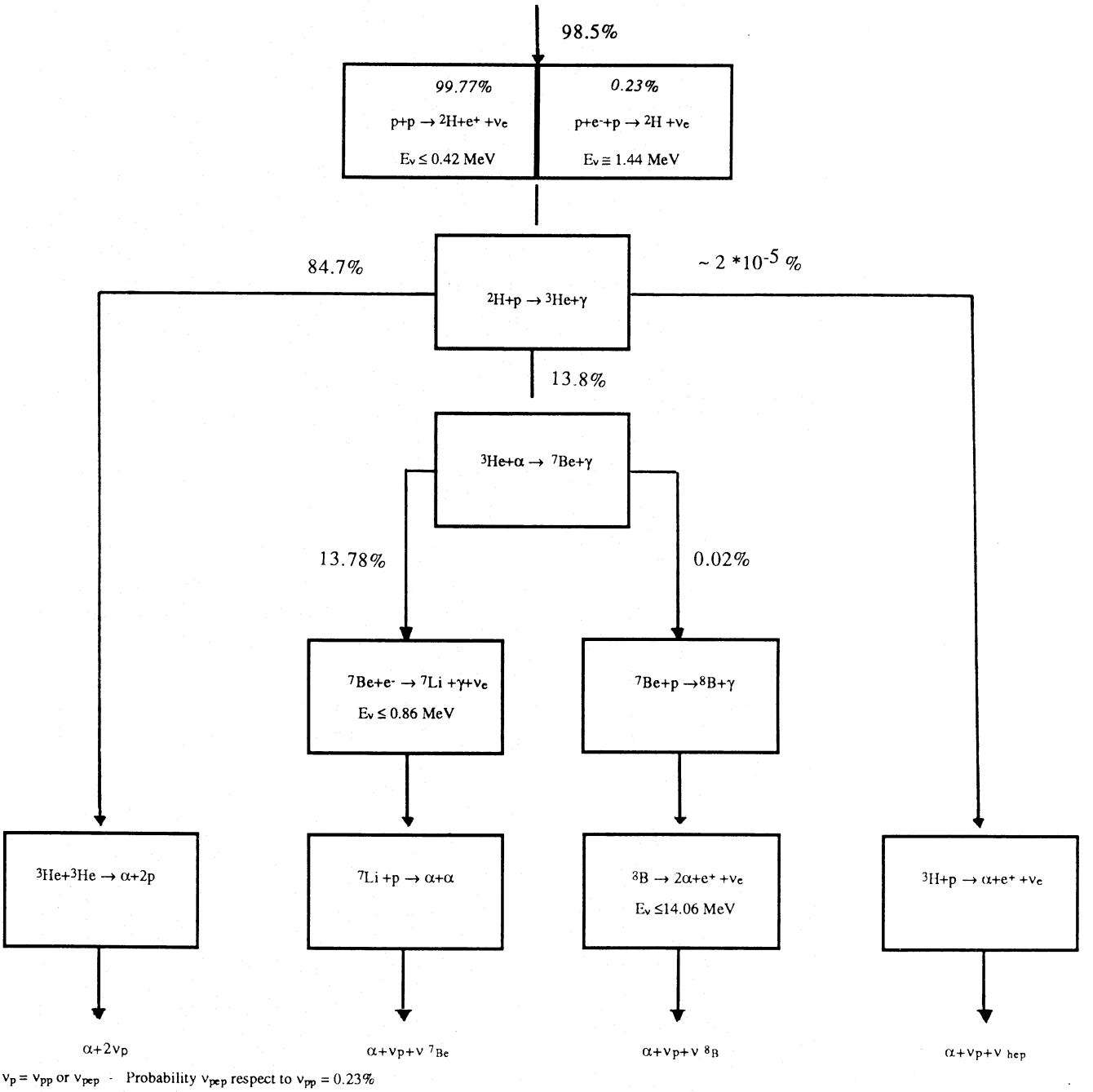

Fig. 2. Nuclear reactions in the p–p chain. For a total probability $P = 98.5\%$ of the pp-chain, we present the calculated probabilities of the various reactions. For the pp and pep neutrino we show, in italics, the relative probabilities

which are, as far as possible, independent of the solar model calculations.

Provided that neutrinos behave conventionally, the signal S^X in a solar neutrino detector X depends on the fluxes Φ_i corresponding to the different branches of the nuclear reactions chain:

$$S^X = \sum_i M_i^X \Phi_i, \qquad (3.1.1)$$

where the matrix M_i^X specifies the detector, i.e. its "response function" for a unitary flux of electron neutrinos with energy spectrum as given by the ith branch of the nuclear reactions chain. Let us remark that we are considering conventional neutrinos, i.e. in the calculation of M_i^X it is assumed that there is no change of lepton number, helicity and energy spectrum during the trip of neutrinos from Sun to Earth. Note also that the energy distribution of these fluxes, $d(\ln \Phi_i)/dE$, is given by well known physics, provided that neutrinos behave conventionally.

Table 2. The strength $\omega\gamma$ of a resonance in the $^3He+^3He$ channel, as a function of the resonance energy E_R. In the second column we present existing experimental upper bounds, from (Krauss et al. 1987) and in the third column the theoretical estimate of the same authors. Our analytical estimate, Eq. (4.3.6) is shown in the fourth column. The results of the calculation by using the FRANEC code are shown in the remaining columns, where $\phi_7=\Phi(^7Be)/\Phi(^7Be)^{SSM}$ and similarly for ϕ_8

E_R (keV)	$\omega\gamma$ Experimental bound (MeV)	$\omega\gamma$ Krauss et al. (1987) (MeV)	$\omega\gamma$ Analytical estimate (MeV)	$\omega\gamma$ FRANEC (MeV)	ϕ_7	ϕ_8
3.0		—	5.6E−22	4.5E−22	0.23	0.30
5.0	—	—	2.6E−21	2.3E−21	0.24	0.30
10.0	—	—	1.3E−19	1.2E−19	0.25	0.30
15.0	—	—	6.0E−18	6.1E−18	0.27	0.30
16.2	≤1.7E−17	1.5E−17	1.5E−17	1.5E−17	0.27	0.30
19.0	≤1.7E−17	1.1E−16	1.3E−16	1.3E−16	0.29	0.30
20.0	≤4.7E−17	—	2.9E−16	2.8E−16	0.30	0.31
21.5	≤1.4E−16	8.3E−16	9.2E−16	1.0E−15	0.30	0.30
24.0	≤5.3E−16	6.3E−15	6.4E−15	7.3E−15	0.32	0.31
27.1	≤5.3E−16	6.5E−14	7.0E−14	8.1E−14	0.34	0.30

In principle, with a suitable series of solar neutrino experiments it is possible to determine the values of all the Φ_i's, by inverting Eq. (3.1.1). The important point is that values of Φ_i extracted in this way have to be consistent among each other, i.e. in the space $\{\Phi_1 \ldots \Phi_n\}$ the planes corresponding to Eq. (3.1.1) have a common crossing point in the physical region ($\Phi_i > 0$). Otherwise, neutrinos are unconventional (i.e. the true M_i^X are different) and/or experiments are wrong.

Since at present we have just two experiments, if we take the experimental results at their face values, we can try to extract two fluxes from the experimental data. For the Kamioka experiment, the analysis is particularly simple. The signal S^K is due to ^8B neutrinos only:

$$S^K = M_B^K \, \Phi(^8B), \tag{3.1.2}$$

where the coefficient M_B^K depends essentially on the $\nu_e + e^- \to \nu_e + e^-$ cross section, which is known to a very high accuracy. The result is generally presented in terms of the ratio with respect to the prediction of the SSM, as calculated by Bahcall & Ulrich (1988):

$$S^K/S^{K(SSM)} = 0.46 \pm 0.05(\text{stat}) \pm 0.06(\text{syst.}). \tag{3.1.3}$$

Thus Kamioka tell us that the ^8B flux is definitely lower than expected from SSM. Since $S^K/S^{K(SSM)} = \Phi(^8B)/\Phi^{(SSM)}$ (^8B) and, according to Bahcall & Ulrich, $\Phi^{(SSM)}$ (^8B) $= 5.8\ 10^6\,cm^{-2}\,s^{-1}$ one can immediately extract the "experimental value" of $\Phi(^8B)$. By summing errors in quadrature, one has

$$\Phi(^8B) = (2.7 \pm 0.4)\ 10^6\ cm^{-2}\,s^{-1}, \tag{3.1.4}$$

where the quoted error corresponds – here and in the following – to $\pm 1\sigma$. We can use Homestake to investigate whether the deficiency in ^8B neutrinos can be ascribed to the (unexpected) dominance of the $^7Be + e^-$ reaction, lowering the production of ^8B neutrinos in favour of ^7Be ones.

The signal in the Homestake experiment,

$$S^H = 2.23 \pm 0.23\ \text{SNU}, \tag{3.1.5}$$

(where 1 SNU $= 10^{-36}$ captures per atom of chlorine per second) can be expressed as the sum of several components of the neutrino flux:

$$S^H = \sum_i M_i^H \, \Phi_i, \tag{3.1.6}$$

where the coefficients M_i^H are given in Table 1, third column. We recall that these coefficients *do not depend* on solar physics. Basically they are determined from the cross section of $\nu_e + {}^{37}Cl \to e^- + {}^{37}Ar$. According to Bahcall, the 1σ errors on the M_i^H are at the level of 2–3%.

As well known, it is expected that the largest contribution to the signal originates from $\Phi(^8B)$, a significant contribution arises from $\Phi(^7Be)$ and a small term, S_{other}, comes from the other components. As discussed in the Appendix, theoretical predictions of available SSMs appear rather similar. From our SSM we find

$$S_B^{SSM} = 6.30(\pm 0.74\ \text{SNU}), \tag{3.1.7}$$

$$S_{Be}^{SSM} = 1.09(\pm 0.05\ \text{SNU}), \tag{3.1.8}$$

$$S_{other}^{SSM} = 0.6(\pm 0.1\ \text{SNU}), \tag{3.1.9}$$

where the estimated uncertainties are from Bahcall (1989), as derived dividing by a factor 3 the "total theoretical uncertainty" quoted in Bahcall's book, since this latter is assumed to correspond to 3σ.

If only the relative efficiency of the two branches originated from ^{7}Be is varied, S_{other} is given by the SSM. Since the flux of ^{8}B neutrinos is much lower than the flux of ^{7}Be neutrinos one expects from Homestake:

$$(S^H - S^{SSM}_{other}) \approx 1.1 + M^H_B \Phi(^8B). \quad (3.1.10)$$

However, if $S_{other} = S^{SSM}_{other}$, Homestake tell us that

$$\begin{aligned}(S^H - S^{SSM}_{other}) &= M^H_B \Phi(^8B) + M^H_{Be} \Phi(^7Be) \\ &= 1.1\ 10^{-6} \Phi(^8B) + 2.35\ 10^{-10} \Phi(^7Be) \\ &= (1.63 \pm 0.23), \end{aligned} \quad (3.1.11)$$

where the fluxes are in units of cm^{-2} s^{-1}. Note that the experimental error is much larger than the uncertainties on M^H_B and M^H_{Be}, so that these latter can be neglected.

We have plotted (see Fig. 3) in the $\{\Phi(^8B), \Phi(^7Be)\}$ plane the regions corresponding to Eqs. (3.1.11) and (3.1.4), at the 1σ level. As well known, one easily recognizes that also the Homestake fluxes are much lower than those predicted by the SSM. No solution shifting the ^{8}B neutrinos in the ^{7}Be branch is allowed (point A), since it is contradicted by Kamioka results. Moreover at 1σ level, there is no intersection between the two experiments, i.e. under the quoted hypothesis on S_{other} it is impossible to determine from the experimental data consistent values of $\Phi(^8B)$ and $\Phi(^7Be)$. Nevertheless, if one allows some "flexibility" in the experimental results, there is room for a nuclear solution in the region marked by the points B and C in the Fig. 3: $\Phi(^7Be) \approx 1/3$–$1/10$ and $\Phi(^8B) \approx 1/3\ \Phi^{SSM}(^8B)$. Note that if S_{other} is larger than assumed, the situation becomes even worse. On the contrary, if $S_{other} < S^{SSM}_{other}$ (as expected e.g. if both CNO and pep burning are totally inefficient) Homestake will progressively approach Kamioka results. The maximum approach is

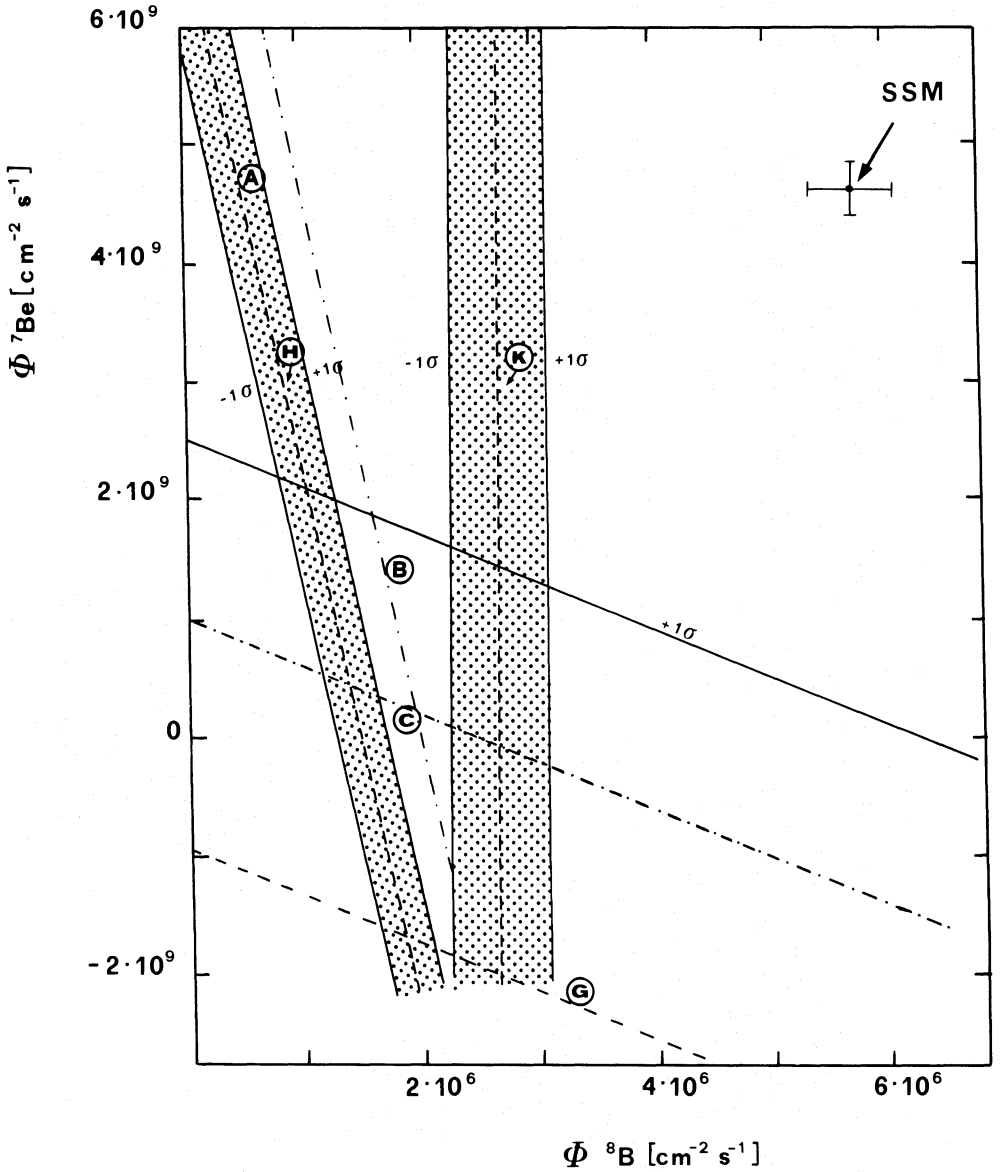

Fig. 3. The information on the ^{7}Be and ^{8}B neutrinos fluxes, as derived from the Homestake (H), the Kamioka (K) and the Gallex (G) experiment. The dashed lines correspond to the central value of the experimental results, full lines denote the 1σ contours. The point (SSM) is the Standard Solar Model prediction, error bars corresponding again to 1σ. Point A corresponds to the solution shifting the ^{8}B neutrinos in the ^{7}Be branch. The region of absolute highest likelihood is labelled as C. Point B corresponds to the highest probability with the constraint that ^{7}Be and ^{8}B neutrino fluxes are equally suppressed. Dashed and dotted lines show the central values for both Gallex and Homestake experiments if S_{other} is taken zero (see text)

obtained if $S_{other}=0$ as shown by the dashed-dotted line in Fig. 3. This would increase the probability of a nuclear solution. As a conclusion, one finds that the only way to keep a nuclear solution is to look for a substantial decrease of both ^{7}Be and ^{8}B neutrino fluxes with respect to the predictions of the standard solar model. Data suggest that the suppression of ^{7}Be neutrinos is even larger than that of ^{8}B neutrinos. One may note that we have considered as Homestake signal the mean value of the experimental results on 20 years; taking only the last experimental data the general agreement would be improved.

The Borexino experiment aims towards a measurement of the ^{7}Be neutrino flux with a high accuracy, thus better locating the results in the plane $\{\Phi(^8B), \Phi(^7Be)\}$. It will be in particular interesting to compare the result with the solution B $\Phi(^7Be)\approx 1.4\ 10^9\ cm^{-2}\,s^1$.

The problem arises, how the region B–C is compatible with our present knowledge of nuclear reactions in stellar interior? This will be discussed in a following section. In the next section we will consider how other solar neutrino experiments can add significant constraints.

3.2. *Gallium experiments*

As well known, the gallium experiments, mostly sensitive to pp neutrinos, are also sensitive to all other neutrinos. We recall that the gallium experiments can really give information which is *absolutely independent* of solar model calculations. It may be worthy to analyze this point in a way which is more explicit than the discussion currently given in the literature (Bahcall et al. 1985).

The idea is that the observed solar luminosity provides a lower bound to the total neutrino flux. The smallest signal is obtained assuming that all these neutrinos are pp neutrinos, since the smaller the energy, the smaller is the detection cross section.

To reach such a conclusion one has only to assume that solar energy originates from hydrogen burning:

$$2e^- + 4p \rightarrow \alpha + 2\nu_e. \tag{3.2.1}$$

If the two neutrinos originate from the ith and jth branch, carrying away energy E_i and E_j respectively, the energy released in the Sun and available to be radiated away is $\Delta E=(Q-E_i-E_j)$, with $Q=2m_e+m_\alpha-4m_p$ $=26.7$ MeV. The radiated energy flux, $K_\odot=1.36\ KW\,m^{-2}$, is thus

$$K_\odot=\sum_i (Q/2-\langle E_i\rangle)\,\Phi_i, \tag{3.2.2}$$

where $\langle E_i\rangle$ is the average energy carried away by neutrinos of the ith branch. Since $\langle E_i\rangle \geq \langle E_{pp}\rangle$, one can derive from Eq. (3.2.2) a bound on the total neutrino flux:

$$\Phi_{tot}=\sum_i \Phi_i \geq \frac{K_\odot}{[Q/2-\langle E_{pp}\rangle]}. \tag{3.2.3}$$

The (positive) coefficients M_i^G relating the Ga-signal with neutrino fluxes,

$$S^G=\sum_i M_i^G \Phi_i, \tag{3.2.4}$$

are ordered according to the average neutrino energy, as a straightforward consequence of the fact that weak interaction cross sections increase with energy, see Table 1. The smallest energy being that of the p–p reaction, one has then

$$S^G \geq M_{pp}^G \Phi_{tot}. \tag{3.2.5}$$

By using Eq. (3.2.3), one gets a lower bound to the signal:

$$S^G \geq M_{pp}^G \frac{K_\odot}{[Q/2-\langle E_{pp}\rangle]}. \tag{3.2.6}$$

The bound corresponds to about 79 SNU for the value of M_{pp}^G given in Table 1, similar to the result of Bahcall et al. (1985).

Note that for deriving this bound we did not even specify which is the cycle relevant for hydrogen burning in the Sun. We only assumed that Sun burns hydrogen into helium, energy is carried out from the Sun at the same rate as it is produced, weak interactions cross sections raise with energy and, of course, we made the hypothesis that neutrinos are conventional.

In addition, one can try to get from gallium experiments further informations, weakly dependent on the Standard Solar Model. As in the previous discussion, let us take from the SSM the (small) contribution of pep, ^{13}N, ^{15}O and ^{17}F, now totalling to about 14 SNU, i.e. 10% of the expected signal in the SSM, 132 SNU. If the fluxes of boron and beryllium neutrinos are different with respect to the SSM calculation, the number of pp neutrinos has to be varied so as to keep constant the total neutrino number, as fixed by the solar luminosity. One can thus isolate the contribution of ^{7}Be and ^{8}B neutrinos in the gallium signal:

$$S^G=(89\pm 2)\,SNU + M_B^G \Phi(^8B) + (M_{Be}^G - M_{pp}^G)\Phi(^7Be). \tag{3.2.7}$$

Errors on the M_{Gi} are estimated to be a few percent. Consistency with the solution B requires a Ga signal of about 103 SNU, whereas the case C corresponds to about 94 SNU. Equation (3.2.7) gives the signal expected in a gallium experiment if both CNO and pep reactions work as in the SSM, i.e. for $S_{other}=S_{other}^{SSM}$. If, on the contrary, $S_{other}^{SSM}=0$ one finds again the already quoted lower bound of ≈ 79 SNU.

The first results of the SAGE collaboration (Abazov et al. 1991),

$$S_G \leq 79\ SNU \quad \text{at } 90\%\ C.L. \tag{3.2.8}$$

pointed against the "nuclear physics" solution. One has to observe, however, that the experimental limit is not terribly severe in this respect, due to the poor statistics collected so far and – most important – in the absence of

the Cr- source calibration. As a matter of the fact, GALLEX collaboration has recently presented the result:

$$S_G = 83 \pm 19\,(\text{stat.}) \pm 8\ (\text{syst.}). \tag{3.2.9}$$

Following the previous discussion, this implies that a nuclear solution cannot be excluded. One can make use of Eq. (3.2.7) to discuss this result in the $\{\Phi(^8B), \Phi(^7Be)\}$ plane. The fact that if $\Phi(^7Be) > 0$, $\Phi(^8B) < 0$ (or vice versa) indicates that, taken at its central value, Gallex result gives too few neutrinos. However, one finds that at 1σ the B–C region appears again as the most probable nuclear solution to the problem of solar neutrinos.

One finally may note that, relaxing the condition on S_{other} one would again find a better agreement among the various experiments, as shown in Fig. 3 by the dashed-dotted line which discloses the Gallex implication for ^7Be and ^8B fluxes if $S_{other} = 0$.

4. The solar neutrino problem, the $^3He + ^3He$ and $^3He + ^4He$ reactions in the Sun

4.1. A scaling law for the equilibrium ^7Be concentration

Differences in the ^7Be and ^8B neutrinos fluxes with respect to the SSM calculations could be attributed – at least in principle – to the values of some nuclear cross sections, which, we recall, have not been measured at the relevant energies. In this respect, there are (at least) three important quantities, the $\langle \sigma v \rangle_{ij}$ at low energies corresponding to $^3He + ^3He$, $^3He + ^4He$ and $p + ^7Be$ reactions.

We have already seen that variations of the rate for the $p + ^7Be$ reaction alone cannot account for the experimental neutrino data, so we will not consider them. Thus, we need to know how the results of the SSM are changed if the $\langle \sigma v \rangle_{33}$ and $\langle \sigma v \rangle_{34}$ are changed. Power laws have been derived by numerical experiments (Bahcall 1989), in the assumption that there are no resonances, i.e. the astrophysical S-factors are smooth, for small variations of the S_i with respect to S_i^{SSM}. These laws cannot be used here, since large variations of the S_i and/or resonant structures are needed in order to explain the neutrino data in terms of modified nuclear cross sections.

In order to estimate the dependence of ^7Be and ^8B neutrinos fluxes on the nuclear cross sections in the general case, let us consider the local equilibrium concentration of the (parent) ^7Be nuclei, n_7. We observe that ^7Be is created in the $^3He + ^4He$ reaction and destroyed, essentially via electron capture, with lifetime τ_{e7}, the proton capture reaction being very unlikely. Thus, at equilibrium:

$$n_7 = \tau_{e7}\, n_3\, n_4 \langle \sigma v \rangle_{34}, \tag{4.1.1}$$

where n_i is the number density of the nucleus with mass number equal to i. The ^3He equilibrium density is obtained by equating its creation rate $(\frac{1}{2} n_1^2 \langle \sigma v \rangle_{11})$ to the burning rate. This latter is dominated by the $^3He + ^3He$ reaction. In fact, in the SSM the $^3He + ^3He$ reaction occurs about six times as often as the $^3He + ^4He$ reaction and in our case (we are considering smaller S_{34} and/or larger S_{33}) this number is even larger, so we neglect the $^3He + ^4He$ channel. In this way we find

$$n_3^2 = \tfrac{1}{2} n_1^2 \frac{\langle \sigma v \rangle_{11}}{\langle \sigma v \rangle_{33}}. \tag{4.1.2}$$

We can now express the ^7Be density, in terms of the H and ^4He densities and of the reaction rates:

$$n_7 = \tau_{e7}\, n_1\, n_4 \frac{\langle \sigma v \rangle_{11}^{0.5} \langle \sigma v \rangle_{34}}{\langle \sigma v \rangle_{33}^{0.5}}. \tag{4.1.3}$$

By changing $\langle \sigma v \rangle_{34}$ and $\langle \sigma v \rangle_{33}$ we only change the termination of the p–p chain and we expect that n_1, n_4 and the temperature T are almost unaffected, since the rate of hydrogen burning (and thus the amount of ^4He which is produced) is mainly determined by the constraints on the Sun age and luminosity.
By defining:

$$x = \frac{\langle \sigma v \rangle_{34}}{\langle \sigma v \rangle_{33}^{0.5}}, \tag{4.1.4}$$

the above equation can be written as

$$n_7 = n_7^{SSM} \frac{x}{x^{SSM}}. \tag{4.1.5}$$

Note that $\langle \sigma v \rangle_{34}$ and $\langle \sigma v \rangle_{33}$ only enter in the combination given by Eq. (4.1.4) and that Eq. (4.1.5) holds locally, i.e. point by point, in the solar interior.

Qualitatively, Eq. (4.1.5) is easily understood. Small values of $\langle \sigma v \rangle_{34}$ (large values of $\langle \sigma v \rangle_{33}$) give a small probability of producing ^7Be. In addition, the dependence on $\langle \sigma v \rangle_{33}$ has to be weaker than on the other parameter, since when $\langle \sigma v \rangle_{33}$ is increased, ^3He is more easily burnt and consequently there is less ^3He available for the $^3He + ^3He$ reaction.

4.2. The non-resonant case

Assuming that there are no resonances at the energies of interest, and only that the low energy astrophysical S-factors differ from the extrapolation used in the SSM ($S_i = s_i S_i^{SSM}$) at any point in the Sun one has

$$\frac{x}{x^{SSM}} = \frac{s_{34}}{\sqrt{s_{33}}}, \tag{4.2.1}$$

and consequently:

$$n_7 = n_7^{SSM} \frac{s_{34}}{\sqrt{s_{33}}}. \tag{4.2.2}$$

The ^7Be and ^8B neutrinos fluxes – which are obviously proportional to n_7 – scale then in the same way:

$$\Phi(^7Be) = \Phi(^7Be)^{SSM} \frac{s_{34}}{\sqrt{s_{33}}}, \qquad \Phi(^8B) = \Phi(^8B)^{SSM} \frac{s_{34}}{\sqrt{s_{33}}}. \tag{4.2.3}$$

It is also natural to assume that the other neutrino fluxes are insensitive to variations of S_{33} and S_{34}:

$$\Phi(\text{other}) = \Phi(\text{other})^{SSM}. \quad (4.2.4)$$

We have verified the validity of Eqs. (4.2.3) and (4.2.4) by using our stellar evolution codes. As S_{34} and S_{33} were varied, the chemical composition of the initial Sun was adjusted (within the existing bounds from the chemical composition of the solar envelope) so as to reproduce the observed solar luminosity for a solar age of 4.6 10^9 yr. The results of the numerical calculations are shown in Figs. 4. Figures 4a, b show the validity of the scaling law in

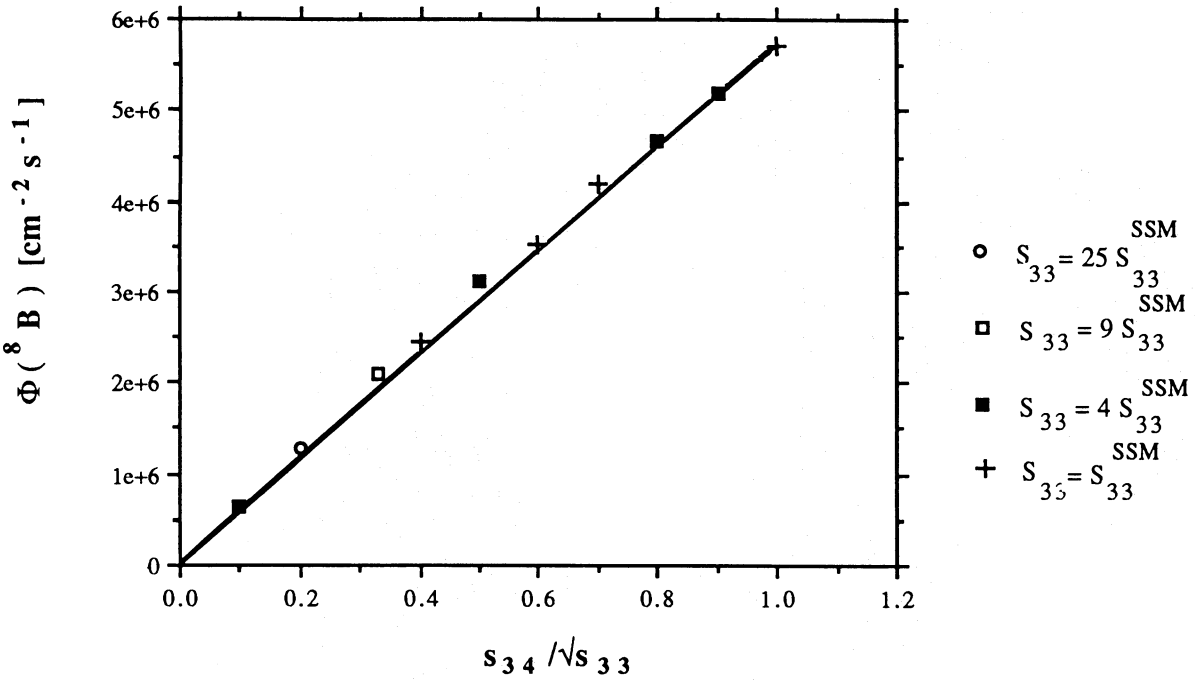

Fig. 4a. The flux of ^{8}B neutrino as a function of $s_{34}/\sqrt{s_{33}}$ for several values of S_{33}, as calculated by using the FRANEC code. The straight line corresponds to Eq. (4.2.3)

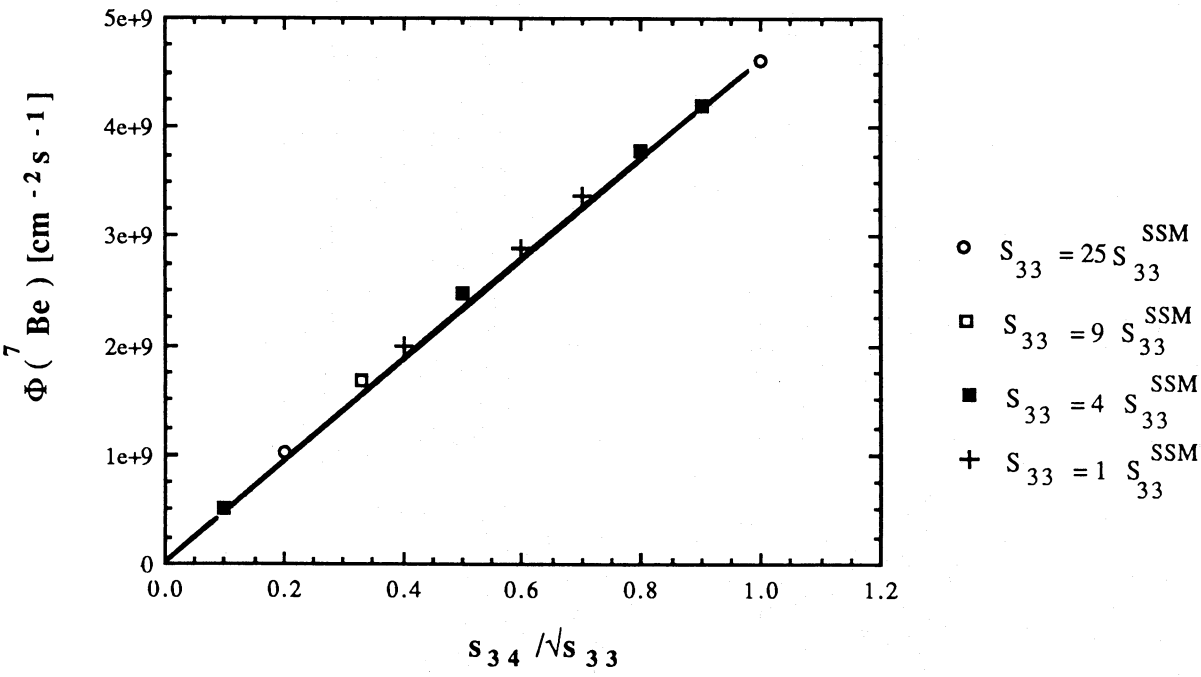

Fig. 4b. Same as above for the ^{7}Be neutrinos

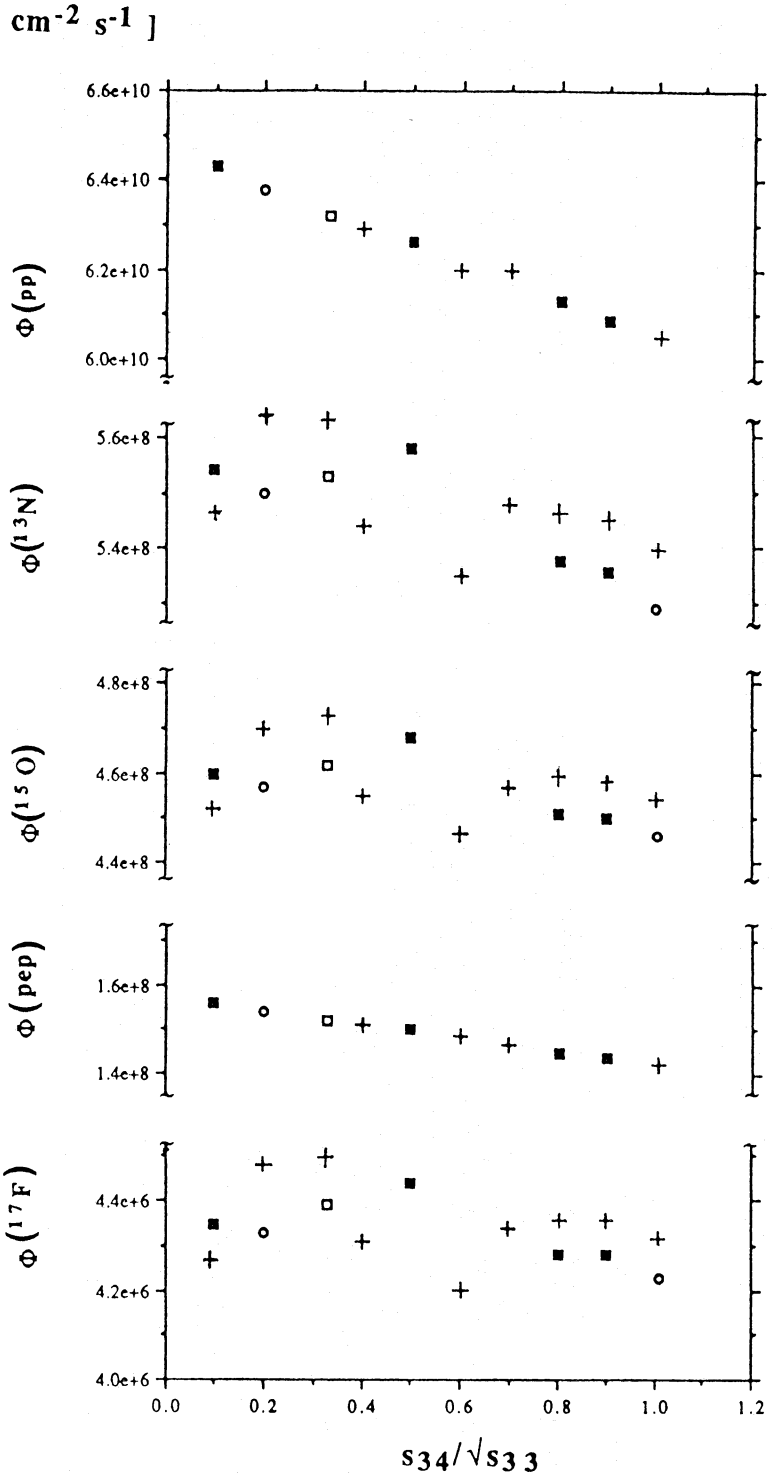

Fig. 4c. Same as above for the other neutrino fluxes

Eq. 4.2.3. It is also worth observing that Eq. (4.2.3) agrees approximately with the dependence estimated by Bahcall (1989) for small variations, $\Phi(^7\mathrm{Be}) = \Phi(^7\mathrm{Be})^{\mathrm{SSM}} s_{34}^{0.86} s_{33}^{-0.43}$ and $\Phi(^8\mathrm{B}) = \Phi(^8\mathrm{B})^{\mathrm{SSM}} s_{34}^{0.81} s_{33}^{-0.40}$.

Concerning Fig. 4c, we note that ^{13}N, ^{15}O and ^{17}F neutrino fluxes stay almost constant. The same holds true for the pp and pep neutrinos, where one notes however a (weak) dependence on the scaling variable $s_{34}/\sqrt{s_{33}}$. This dependence can be easily understood by observing that the total flux $[\Phi_{\mathrm{tot}} \cong \Phi(\mathrm{pp}) + \Phi(\mathrm{pep}) + \Phi(^7\mathrm{Be})]$ is essentially fixed by the observed solar luminosity, and that the ratio $\Phi(\mathrm{pep})/\Phi(\mathrm{pp})$ is unaltered as s_{33} and s_{34} are

varied. If $\Phi(^7\mathrm{Be})$ is reduced both $\Phi(\mathrm{pp})$ and $\Phi(\mathrm{pep})$ have to be accordingly increased, thus:

$$\Phi(\mathrm{pp}) = \Phi^{\mathrm{SSM}}(\mathrm{pp}) \left\{1 + \left(1 - \frac{S_{34}}{\sqrt{S_{33}}}\right) \frac{\Phi^{\mathrm{SSM}}(^7\mathrm{Be})}{[\Phi(\mathrm{pp}) + \Phi(\mathrm{pep})]^{\mathrm{SSM}}}\right\}$$

and similarly for $\Phi(\mathrm{pep})$. From our calculations $\Phi^{\mathrm{SSM}}(^7\mathrm{Be})/[\Phi(\mathrm{pp}) + \Phi(\mathrm{pep})]^{\mathrm{SSM}} = 0.075$. A linear fit of the numerical results yields for this slope the value 0.067 for both $\Phi(\mathrm{pep})$ and $\Phi(\mathrm{pp})$.

Clearly, in the case we are discussing, the ^{7}Be and ^{8}Be neutrinos fluxes are reduced in the same way. Following the discussion of the previous section, the neutrino data could be accounted for if $S_{34}/\sqrt{S_{33}}$ at low energy is about one third with respect to the present estimate, i.e. S_{34} should be wrong by a factor three or S_{33} wrong even by an order of magnitude, or some mixed combinations.

By looking at the data taken so far (see Figs. 5 and 6), this situation looks unlikely, at least as long as the astrophysical factors have a relatively gentle behaviour.

4.3. A resonance in the $^3He + ^3He$ channel?

This possibility, first advanced in Fowler (1972), cannot be completely dismissed, see the discussion in Rolfs & Rodney (1988). Let us analyze this possibility in some detail, as we expect that future experiment can add significant information. We consider, of course, a narrow resonance, otherwise its (higher energy) tail should have been detected in previous experiments.

The starting point for the discussion is again the expression for the local concentration of ^{7}Be nuclei, Eq. (4.1.5), which we write as:

$$n_7 = n_7^{\mathrm{SSM}}[\langle\sigma v\rangle_{33}^{\mathrm{SSM}}/\langle\sigma v\rangle_{33}]^{0.5}. \tag{4.3.1}$$

Assuming that the resonance dominates over the background given by the SSM, $(\langle\sigma v\rangle_{33} = \langle\sigma v\rangle_{33}^{\mathrm{SSM}} + \langle\sigma v\rangle_{33}^{\mathrm{res}} \approx \langle\sigma v\rangle_{33}^{\mathrm{res}})$ we can write:

$$n_7 = n_7^{\mathrm{SSM}} \frac{(\mu\Delta S_{\mathrm{eff}})^{1/2}}{(2\pi^{3/2}h^2\omega\gamma)^{1/2}} \mathrm{e}^{\frac{-3E_0(kT)+E_{\mathrm{R}}}{2KT}}, \tag{4.3.2}$$

where E_{R} and $\omega\gamma$ are the resonant position and strength respectively. $E_0(kT)$ is the Gamow energy for the ^{3}He–^{3}He reaction, S_{eff} is the effective astrophysical S-factor at the temperature T (Rolfs & Rodney 1988), $E_0 = A(kT)^{2/3}$ with $A = 1.804\ \mathrm{MeV}^{1/3}$ ($E_0 = 21.97$ keV for a central solar temperature $T_c = 15.6\ 10^6$ K) and the other quantities are defined as usually, see for example Rolfs & Rodney (1988).

The quantity which is mostly sensitive to the temperature T is clearly the exponential term, whereas Δ and S_{eff} are weakly variable. Neglecting the temperature dependence of these quantities, we write Eq. (4.1.5) as

$$n_7 = n_7^{\mathrm{SSM}}(W/\omega\gamma)^{1/2} \exp[-3/2A(kT)^{-1/3} + 1/2E_{\mathrm{R}}(kT)^{-1}], \tag{4.3.3}$$

with

$$W = \frac{(\mu\Delta S_{\mathrm{eff}})^{1/2}}{(2\pi^{3/2}h^2)^{1/2}} = 20.4\ \mathrm{keV}.$$

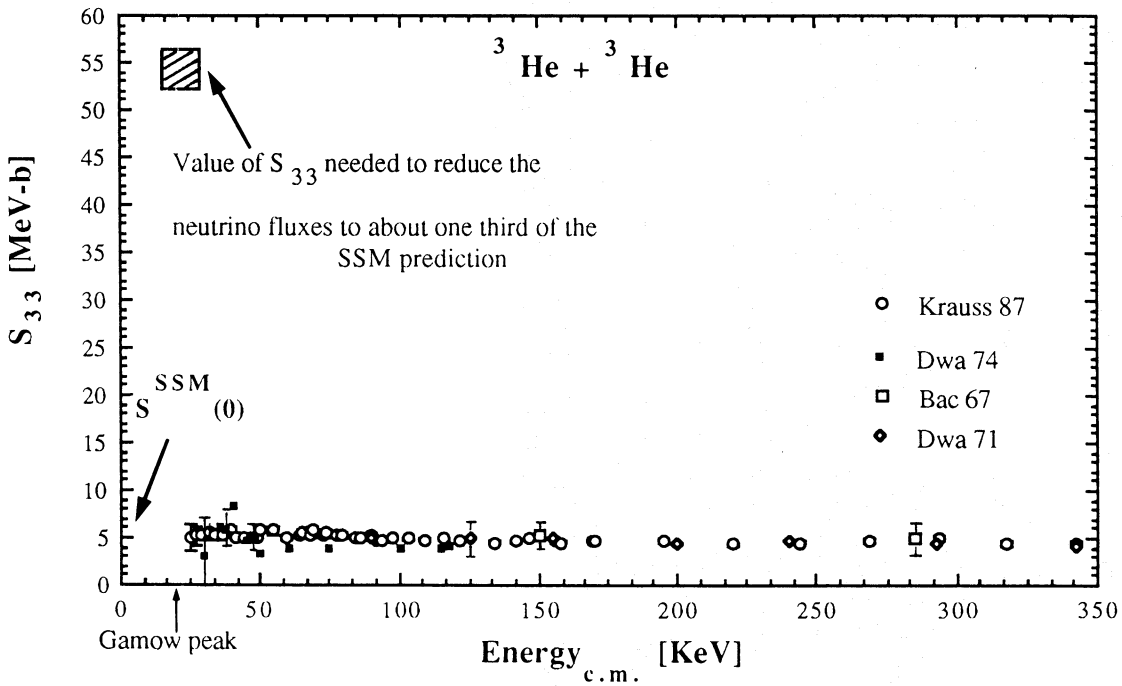

Fig. 5. The available experimental data for S_{33} as reported in Rolfs & Rodney (1988) and in Krauss et al. (1987). The extrapolated value used in SSM calculations is $S_{33}^{\mathrm{SSM}}(0) = 5.15$ MeV b. The shaded area corresponds to the value of S_{33} which is needed in order to reduce the neutrino fluxes to about one third of the SSM prediction

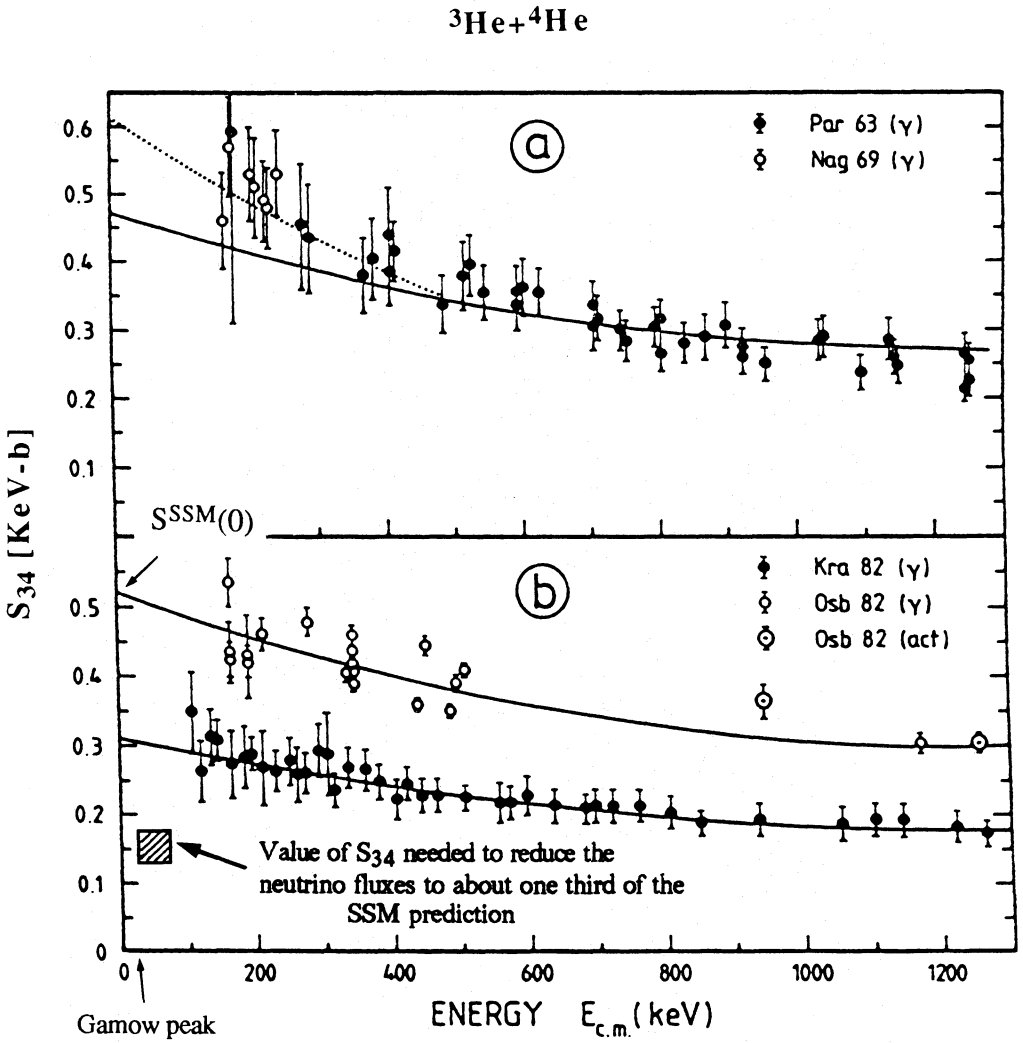

Fig. 6. The available experimental data for S_{34}, from (Rolfs & Rodney 1988). Note in (b) two sets of data inconsistent between each other. The extrapolated value generally used in SSM calculations is $S_{34}^{SSM}(0) = 0.54$ keV b. The shaded area corresponds to the value of S_{34} which is needed in order to reduce the neutrino fluxes to about one third of the SSM prediction

The fluxes of ^{7}Be and ^{8}B neutrinos are obtained by averaging n_7 over the respective production regions. As a simplification, we assume that the fluxes are proportional to n_7 calculated in the region of maximal production, i.e.

$$\frac{\Phi(^8\mathrm{B})}{\Phi^{SSM}(^8\mathrm{B})} = \frac{n_7(T_B)}{n_7^{SSM}(T_B)}, \qquad T_B = 15\ 10^6\ \mathrm{K}, \tag{4.3.4}$$

$$\frac{\Phi(^7\mathrm{Be})}{\Phi^{SSM}(^7\mathrm{Be})} = \frac{n_7(T_{Be})}{n_7^{SSM}(T_{Be})}, \qquad T_{Be} = 14.5\ 10^6\ \mathrm{K}. \tag{4.3.5}$$

By requiring that the resonant rate is ten times the SSM prediction for the non resonant component (so that the ^{8}B neutrino flux is 0.3 with respect to the SSM prediction) we derive from the above equation a relation between the resonance strength and the resonant energy:

$$\omega\gamma = 10\,W\,e^{-3A(kT_B)^{-1/3} + E_R(kT_B)^{-1}}. \tag{4.3.6}$$

The numbers we find are quite similar to the estimate of Krauss et al. (1987), see Table 2. By using the FRANEC stellar evolution code we have found the resonance parameters such that $\Phi(^8\mathrm{B})/\Phi^{SSM}(^8\mathrm{B}) = 0.3$. These values agree with the analytical estimate given above, see again Table 2. The available experimental results, also reported in Table 2, seem to exclude a resonance with a sufficient strength for $E_R \geq 18$ keV.

We remark that, as the production regions correspond to different (effective) temperatures, the suppressions of ^{7}Be and ^{8}B neutrinos with respect to the SSM prediction can be different. As already noted, data indicate that the suppression of $\Phi(^7\mathrm{Be})$ is larger than that of $\Phi(^8\mathrm{B})$. Thus the function in the exponential of (4.3.3) has to be decreasing as the temperature decrease from T_B to T_{Be}. By defining $\phi_7 = \Phi(^7\mathrm{Be})/\Phi^{SSM}(^7\mathrm{Be})$ and similarly ϕ_8 and expanding the exponential around T_c one has

$$\frac{\phi_7}{\phi_8} = e^{-\frac{kT_B - kT_{Be}}{kT_B} 1/2 \frac{E_0(kT_B) - E_R}{kT_B}}. \tag{4.3.7}$$

By requiring $\phi_7 \leq \phi_8$ one gets a condition on the resonance energy:

$$E_R \leq A(kT_B)^{2/3} = 21.4\ \mathrm{keV}. \tag{4.3.8}$$

Thus only a very low energy resonance can account for the fact that ^{7}Be neutrinos are more suppressed than ^{8}B neutrinos.

The (relative) suppression of ϕ_7 with respect to ϕ_8 can be calculated by using Eq. (4.3.7). (We show in Table 2 also the values of ϕ_7 and ϕ_8 calculated by using the FRANEC code, which are in good agreement with the analytical estimate). Note that ϕ_7/ϕ_8 is maximal for $E_R = 0$ where one has $\phi_7/\phi_8 = 0.76$.

In conclusion, the experimental study of the lowest energy region is most important. We note that the experimental upper bound $\omega\gamma \leq 1.7\ 10^{-17}$ MeV at the lowest region so far accessible, $E \approx 18$ keV is mainly due to the natural background in the laboratory. Preliminary estimates show that this background can be reduced by a factor about 100 by working in an underground laboratory. One expects that the limiting $\omega\gamma$ is correspondingly decreased. In conclusion, see Fig. 7, experiments in underground laboratory will have sufficient sensitivity so as to explore the region of resonance down to $E_R = 10$ keV, which represents a substantial improvement with respect to the present situation.

Note, however, that ϕ_7/ϕ_8 cannot be reduced below 0.76 due to the resonance effect. In this respect the direct measurement of ϕ_7, as planned in the Borexino experiment, and the comparison with ϕ_8, as given by the Kamioka experiment, can be a crucial test for the resonance mechanism.

5. Conclusions

(i) With the aim of estimating which space is still left for a nuclear physics solution of the solar neutrino problem, we have discussed the data of the Kamioka and Homestake experiments, assuming only that (a) the SSM gives the correct prediction for the (small) signal corresponding to ^{13}N, ^{15}O and pep neutrinos and (b) neutrinos behave conventionally. We find that it is not easy to extract from the data consistent values of both the ^{8}B and ^{7}Be neutrino fluxes, see Fig. 3. Consistency can only be obtained – however with a small probability – provided that both ^{8}B and ^{7}Be neutrino fluxes are reduced by a substantial factor with respect to the predictions of the SSM. Furthermore, the data suggest that the suppression of ^{7}Be neutrinos is even larger than that of ^{8}B neutrinos.

(ii) In order to study the sensitivity of the ^{8}B and ^{7}Be neutrino fluxes to the behaviour of the ^{3}He+^{3}He and ^{3}He+^{4}He cross sections, we have analytically derived a scaling law for the local ^{7}Be equilibrium concentration,

$$n_7 \propto \frac{\langle \sigma v \rangle_{34}}{\langle \sigma v \rangle_{33}^{0.5}},$$

which can be used for a large range of the extrapolated astrophysical factors and/or in the presence of resonances.

(iii) In the non-resonant case, reduction of the neutrino fluxes to about 1/3 of the SSM could be obtained if the true value of $S_{34}(0)$ is three times smaller than the presently accepted extrapolated value, a situation which looks unlikely, see Fig. 6, although some inconsistency among experimental values exists. Alternatively, one should have $S_{33}(0)$ wrong by a factor nine, which looks as extremely unlikely, see Fig. 5.

(iv) A resonance in the ^{3}He+^{3}He channel could yield a suppression of ^{7}Be neutrinos larger than that of ^{8}B neutrinos provided that $E_R \leq 21.4$ keV, an energy region essentially unexplored in previous experimental searches.

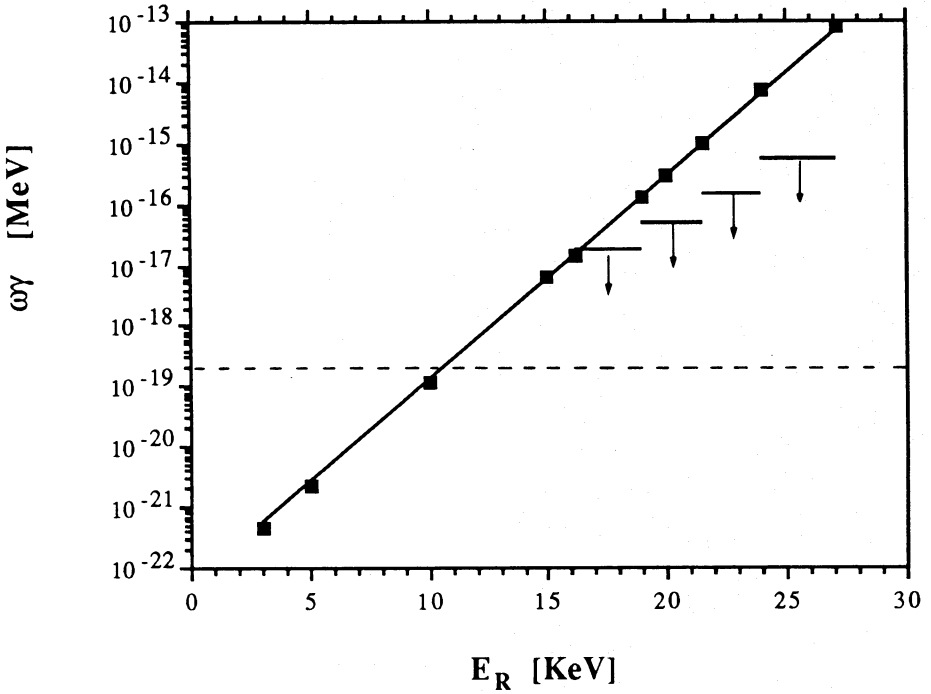

Fig. 7. The strength $\omega\gamma$ of the ^{3}He+^{3}He resonance as a function of resonance energy, such as to obtain $\Phi(^8\text{B}) = 0.30\ \Phi^{\text{SSM}}(^8\text{B})$, as derived from the analytical estimate (full line, see Eq. 4.3.6) and from the FRANEC code (squares). The arrows correspond to the experimental upper bounds on the strength, from (Krauss et al. 1987). The dashed line corresponds to the sensitivity which can be obtained in underground experiments

(v) Provided that the background can be reduced by a factor hundred with respect to sea level – as indicated by preliminary estimates (Arpesella et al. 1991) – future experiments in underground laboratories can explore the region down to $E_R = 10$ keV with a significant sensitivity.

(vi) Our scaling laws and other analytical estimates have been verified by using the FRANEC stellar evolution code. The solar neutrino fluxes corresponding to our Standard Solar Model are quite similar to the values calculated by Bahcall & Ulrich (1988) and by Sackmann et al. (1990), see Table A6 for a comparison. As all other authors, we used the Los Alamos opacity tables. Recently the opacity values of Livermore (Iglesias & Rogers 1991) became available to us. By using these inputs, the ^{8}B and ^{7}Be neutrino fluxes increase by 20% and 10% respectively (see Appendix), leaving the problem of solar neutrinos practically unaltered.

After this paper was completed, we received a preprint by Bahcall & Pinsonneault (1992), where several Standard Solar Models are compared, and the effect of the Livermore opacities is also considered. We fully agree with that paper. Moreover from Table A3 one may notice that our neutrino fluxes tend to be a bit lower of the fluxes given by Bahcall (1988). However comparison with new data in the preprint where the adopted equation of state (EOS) has been improved by including Coulomb interactions of the plasma or intermediate screening, shows a better agreement. Comparison of our SSM with Livermore opacities with models given by Bahcall & Pinsonneault (1992) shows a general good agreement with our fluxes tending to be a bit larger. Also our evaluation of the original helium abundance appears larger by about $\Delta Y = 0.02$. In our opinion the origin of such differences should be likely attributed to the different equation of state and may be to differences in the range of temperature covered by the adopted Livermore opacities. Further comparison about the origin of such differences can be interesting in the future. However one has to remind that we are still waiting to be able to compute a SSM with an EOS fully compatible with the adopted opacity tables.

Acknowledgements. It is a pleasure to thank I. Mazzitelli for kindly providing us with the code handling Livermore opacities and R. Barbieri for several fruitful discussions.

Appendix: the standard solar model

A.1. The code

To obtain a standard solar model one needs evaluate the structure of a new-born Sun, thus following the time evolution of this structure for the canonical 4.6 billion years. To perform such evolutionary computations we adopted the Frascati Raphson Newton Evolutionary Code (FRANEC) which has been already successfully tested for a long time and over a very large range of both stellar masses and evolutionary stages (see e.g. Chieffi & Straniero 1989; Castellani et al. 1991, 1992). This makes us rather confident both in the code and in the adequacy of the physical inputs. As a matter of fact, the advanced phases of stellar evolution become progressively more and more dependent on even minor variations either in the computational scheme or in the evaluation of physical quantities. The success of the quoted tests suggests that the code can be safely used to follow a rather simple evolution as the solar evolution is.

The code FRANEC has been already described in previous papers (see e.g. Chieffi & Straniero 1989); here we will only recall some general features which can be of interest for comparison with previous computations of solar model. Not discussed features are in general as in Bahcall (1989).

A.1.1. Computational procedures

The number of meshes in mass throughout the structure is determined by the program under the condition that all along the evolution of the model neither the physical quantities nor the chemical composition vary between two consecutive meshes more than a prefixed percentage quantity. Our experience shows that a number of meshes around 220 appears adequate for a detailed description of the solar structure.

Time steps are again determined by the program, under the condition of a maximum percentage variation of the value of both physical and chemical quantities in all meshes between two successive models. In such a way we find that about 130 time-steps are needed to follow the solar evolution till the present Sun.

Time evolution of the chemical composition in radiative layers is followed through a Newton Raphson implicit scheme, working on the network of nuclear reactions concerning the pp chain and the CN–NO bicycle. During the convective episode at the beginning of solar evolution the evolution of nuclear species in the convective core has been evaluated through a first-order Taylor expansion (see Chieffi & Straniero 1989).

A.1.2. Physical inputs

For the equation of state (EOS) we consider two separate region: a high-temperature region ($T > 10^6$ K), where matter can be assumed as completely ionized and a low temperature region ($T < 10^6$ K) where partial ionization may take place. In high-temperature region we used the EOS of Straniero (1988) which include Coulomb interactions among ions and electrons. In the low temperature region, the thermodynamical properties of partially ionized matter are derived from the Saha equation. The partial ionization of H is taken into consideration together with He, an average metal, and the H_2 molecule; the pressure ionization is included according to the method described by Ratcliff (1987).

For the solar composition and the relative evaluation of radiative opacity coefficient we used two alternative assumptions. For a better comparison with previous SSM, the first set of models has been computed on the basis of Los Alamos Opacity Library (Huebner et al. 1977) assuming the solar composition from Ross & Aller (1976). Since LAOL opacities do not extend to temperature lower than 10^4 K, below such a temperature we adopted the Cox & Tabor (1976) tables. However, our best model has been finally produced assuming a solar composition as in Anders & Grevesse (1989) (photospheric mixture), with the corresponding Livermore opacity evaluations (Iglesias & Rogers 1991), implemented below (6000 K) with Kurucz's ATLAS8 evaluation. In all case the solar Z/X is from Grevesse (1984): $Z/X = 0.0276$.

The nuclear reaction rates are as in Bahcall (1989) but with new values (Caughlan & Fowler 1988) for $C^{12}(p, \gamma)$ N^{13}, $C^{13}(p, \gamma)$ N^{14}, and for $N^{15}(p, \alpha)$ C^{12}. Table A1 compares the nuclear reaction rates used in this paper (CDF) with the values used in selected previous standard solar model calculations. The only relevant differences are in the value of $S(0)_{33}$ adopted by Sackmann et al. (1990) and Turck-Chièze et al. (1988) and in the value for the $Be^7(p, \gamma)B^8$ cross section used by Turck-Chièze et al. Regarding $S(0)_{33}$ we follow, according to Bahcall (1989), the analysis of Parker (1986) and we adopt $S(0)_{33} = 5.15 \pm 0.09$ MeV barns. For $S(0)_{17}$ we adopt the value suggested by Rolfs & Rodney (1988), which agrees with the rate published by Caughlan & Fowler (1988). Electron screenings (including intermediate screening) are from Graboske et al. (1973) (see also DeWitt et al. 1973).

A.2. The procedure

In order to produce our solar standard model, zero age main sequence models with solar mass and solar metallicity (Z/X) have been evolved through the phase of central H burning for various assumptions about the amount of original helium (Y). The evolutionary sequence producing the solar model is that reproducing the parameters of the real Sun: $L_\odot = 3.826(8)\ 10^{33}$ erg s^{-1} (Astronomical Almanac for the year 1990), $R = (6.960 \pm 0.0007)\ 10^{10}$ cm (Allen 1963) at the solar age ($t = 4.6\ 10^9$ yr). We made certain that our models were within about a tenth of a percent of these

Table A1. The low energy astrophysical factors and their first derivatives for the nuclear reactions of pp chain and CNO bi-cycle adopted in our SSM (CDF), and in selected previous solar standard models: Bahcall 1989 (Bahcall), Turck-Chièze et al. 1988 (Turck–Chièze) and Sackmann et al. 1990 (Sackmann). The units of $S(0)$ and $S'(0)$ are respectively MeV barns and barns

	CDF	Bahcall	Turck-Chièze	Sackmann
pp chain				
$S(0)$ pp	4.07E−25	4.07E−25	4.07E−25	4.07E−25
$S'(0)$ pp	4.52E−24	4.52E−24	4.52E−24	4.52E−24
$S(0)$ 33	5.15E+00	5.15E+00	5.57E+00	5.57E+00
$S'(0)$ 33	−9.00E−01	−9.00E−01	—	−8.24E+00
$S(0)$ 34	5.40E−04	5.40E−04	5.40E−04	5.40E−04
$S'(0)$ 34	−3.10E−04	−3.10E−04	—	—
$S(0)$ 17	2.43E−05	2.43E−05	2.10E−05	2.40E−05
$S'(0)$ 17	−3.00E−05	−3.00E−05	—	—
CNO cycle				
$S(0)$ 12C+p	1.40E−03	1.45E−03	—	1.40E−03
$S'(0)$ 12C+p	4.24E−03	2.45E−03	—	4.24E−03
$S(0)$ 13C+p	5.77E−03	5.50E−03	—	5.77E−03
$S'(0)$ 13C+p	1.40E−02	1.34E−02	—	1.40E−02
$S(0)$ 14N+p	3.32E−03	3.32E−03	—	3.20E−03
$S'(0)$ 14N+p	−5.91E−03	−5.91E−03	—	−5.91E−03
S(0) 15N+p16O+G	6.40E−02	6.40E−02	—	6.40E−02
S'(0) 15N+p16O+G	3.00E−02	3.00E−02	—	3.00E−02
S(0) 15N+p12C+A	7.04E+01	7.80E+01	—	7.04E+01
S'(0) 15N+p12C+A	4.21E+02	3.51E+02	—	4.21E+02
$S(0)$ 16O+p	9.40E−03	9.40E−03	—	9.40E−03
$S'(0)$ 16O+p	−2.30E−02	−2.30E−02		

values at the solar age ($\pm 5\ 10^7$ yr). The ratio Z/X of solar metallicity to solar hydrogen abundance by mass (which affects the evolution of the Sun mainly owing to his influence on opacity) is fairly well determined by observations; our adopted value is taken from Grevesse (1984). Generally one quotes a standard deviation of about 6% for this quantity (Bahcall & Ulrich 1988). The fact that Z/X is fixed for solar models implies that the initial content of helium and heavy elements cannot be chosen independently: if the helium content increases, the metallicity must decrease, for Z/X remaining at his observed value. As well known, increasing the original content of helium the age of the model reaching the right luminosity decreases. Tuning the amount of original helium to obtain the solar luminosity after 4.6 billion years (Bahcall 1989) we found the correct value of Y. The right solar radius is finally found

Table A2. Comparison of our sun (CDF) with some of the most recent standard models given in the literature: Bahcall (1989) (Bahcall), Turck-Chièze et al. (1988) (Turck-Chièze) and Sackmann et al. (1990) (Sackmann). ρ_c, T_c P_c, T_b, ρ_b, pp and CNO means, respectively density, temperature and pressure to the centre, temperature, density and pressure to the base of the convective envelope, fraction of luminosity that originates in the pp chain and in the CNO cycle

Parameter	CDF	Bahcall	Turck-chièze	Sackmann
Y	0.284	0.271	0.276	0.278
Z	0.0192	0.0196	0.0197	0.0194
$M_\odot$	1.989E+33 g	1.989E+33 g	1.989E+33 g	1.989E+33 g
Z/X	0.0276	0.0276	0.0280	0.0277
$L_\odot$	3.83E+33 erg s^{-1}	3.86E+33 erg s^{-1}	3.86E+33 erg s^{-1}	3.86E+33 33 s^{-1}
age	4.6E+9 yr	4.6E+9 yr	4.6E+9 yr	4.54E+9 yr
$R_\odot$	6.96E+10 cm	6.96E+10 cm	6.96E+10 cm	6.96E+10 cm
$T_{\text{effective}}$	5768 °K	5772 °K	5770 °K	—
ρ_c	151 g cm^{-3}	148 g cm^{-3}	148 g cm^{-3}	147 g cm^{-3}
T_c	1.56E+7 K	1.56E+7 K	1.55E+7 K	1.54E+7 K
P_c	2.34E+17 dyn cm^{-2}	2.29E+17 dyn cm^{-2}	2.28E+17 dyn cm^{-2}	—
Central hydrogen (by mass)	0.34	0.34	0.35	0.36
Depth convective zone	$0.016M_\odot$	$0.015M_\odot$	$0.019M_\odot$	$0.017M_\odot$
T_b	2.11E+6 K	1.92E+6 K	2.04E+6 K	1.96E+6 K
ρ_b	0.12 g cm^{-3}	0.12 g cm^{-3}	0.153 g cm^{-3}	0.137 g cm^{-3}
pp	0.986	0.984	—	—
CNO	0.014	0.016	—	—
α	1.6	—	1.55	2.1

Table A3. Comparison of our results (CDF) about the predicted flux (cm^{-2} s^{-1}) of neutrinos with results obtained from the solar model reported in Table A2. The remainder columns give the capture rates predicted for the ^{37}Cl detector in units of SNU (1 SNU = 10^{-36} captures per atom of chlorine s^{-1}). The central temperature (T_c) and the age of the models are also indicated. This calculation corresponds to Los Alamos opacities

	Φ CDF T_c=1.56E+7 K Y=0.284, Z=0.0292 Age=4.6E+9 yr	Φ Bahcall T_c=1.56E+7 K Y=0.271, Z=0196 Age=4.6E+9 yr	Φ Turck-Chièze T_c=1.55E+7 K Y=0.276, Z=0.0197 Age=4.6E+9 yr	Φ Sackmann T_c=1.54E+7 K Y=0.278, Z=0.0194 Age=4.5E+9 yr	CDF (SNU)	Bahcall (SNU)
pp	6.1E+10	6.0E+10	6.0E+10	6.0E+10	0	0
7Be	4.6E+09	4.7E+09	4.2E+09	4.2E+09	1.1	1.1
13N	5.4E+08	6.1E+08	—	4.0E+08	0.1	0.1
pep	1.4E+08	1.4E+08	1.3E+08	1.3E+08	0.2	0.2
15O	4.5E+08	5.2E+08	—	3.1E+08	0.3	0.3
17F	4.3E+06	5.2E+06	—	4.2E+06	0.003	0.004
8B	5.7E+06	5.8E+06	3.8E+06	5.8E+06	6.3	6.1
hep	7.5E+03	7.6E+03	—	6.5E+03	0.03	0.03

tuning the mixing length parameter governing the efficiency of external convection (the convective envelope of our standard Sun comprises the outer 1.6% of the solar mass).

A.3. The results

Table A2 compares our Sun with some of the most recent solar standard models given in the literature. In general all recent papers indicate a presolar helium content in the range $0.271 \leq Y \leq 0.285$ at the Grevesse (1984) value of Z/X. We have checked that the slight differences in the solar age, solar luminosity and Z/X assumed by different authors (see Table A2) have negligible effect on the Sun evolution and therefore on the neutrino rate production. The different values of α are due to the differences in adopted molecular opacities but this does not seem to affect conditions at the base of the solar convective envelope (see Sackmann et al. 1990).

Table A3 compares our results about the flux of neutrinos with similar results obtained from the solar standard models shown in Table A2. As a whole one finds a general agreement among the various computations. In fact, as well known, the efficiency of nuclear reactions for a star is determined by the need to compensate the radiation losses; the constraint that a solar model reaches the solar luminosity at the solar age determines his central conditions (if the nuclear cross sections are fixed) and therefore the production of neutrinos from the various channels. The only sizeable difference is the lower value predicted by Turck-Chièze for the ^{8}B neutrinos. As described by the same author (1992) this discrepancy was due to opacity inconsistencies in the calculations (1/3), to the adopted value of $S(0)_{17}$ (1/3) and to the use of intermediate electron screening in the computation (the last 1/3).

One may note that our Los Alamos-SSM, though using intermediate screening factors, is regaining Bahcall's value for $\Phi(^8\mathrm{B})$. Analytical evaluations, supported by numerical experiments on our model, fully confirm Turck-Chièze's estimates about the influence of $S(0)_{33}$ and $S(0)_{17}$, so that one may conclude that our fluxes is further increased by small differences in the physical input, likely in the EOS.

Table A4 finally compares our previous SSM with a similar model computed adopting the recent Livermore's opacity. Following the already described procedure one finds for this "revised" SSM: $Y=0.295$, $Z=0.0190$, $\alpha=1.87$. As shown in the table, the new opacity runs in the sense of increasing the flux of ^{8}B neutrinos up to about 20%. The reason is rather simple: for the solar interior the Livermore opacity is larger than the Los Alamos opacity by a factor of order 10%, this implies a larger gradient of temperature, shifting the energy production toward the hotter central region. As a result, one finds that the new opacities go in the wrong direction, increasing the discrepancy with experiments. The use of "Los Alamos" SSM throughout all the paper has been suggested to allow a clear comparison with previous works, handling neutrino fluxes usually found in the literature. However, we present in Table A5 our "Livermore" SSM as the more up-to-date evaluation of the Sun we can give with present physics.

Table A4. Neutrino fluxes for our solar standard model ($cm^2\ s^{-1}$) with Los Alamos and Livermore opacity. The central temperature (T_c) and the value of the mixing length parameter (α) are also reported

	Φ Los Alamos opacity $T_c=1.56E+7$ K $Y=0.284$, $Z=0.0192$ $\alpha=1.6$	Φ Livermore opacity $T_c=1.57E+7$ K $Y=0.295$, $Z=0.0190$ $\alpha=1.87$
pp	6.06E+10	6.03E+10
7Be	4.64E+09	5.06E+09
13N	5.40E+08	4.81E+08
pep	1.43E+08	1.40E+08
15O	4.54E+08	4.20E+08
17F	4.33E+06	5.22E+06
8B	5.73E+06	6.93E+06
hep	7.54E+03	7.34E+03

Table A5. Physical and chemical characteristics of our standard solar model with the Livermore opacity. For the solar interior from left to the right the columns give: the mass included in the current and all inner zone, in units of $M_\odot$, (M/M_t), the radius in units of $R_\odot$ (R/R_t), the logarithm of the pressure in units of dyn cm^{-2} (log P), the logarithm of the temperature in K (log T), the logarithm of the density in g cm^3 (log ρ), the luminosity integrated up to and including the current zone in units of $L_\odot$ (L/L_{sup}), the rate of energy production in the zone in erg/g (ε_{nuc}), the flux of pp, ^{7}Be, ^{8}B neutrinos in cm^{-2} s^{-1}, the radiative gradient (G_{rad}), the hydrogen abundance, by mass, (H), the value of the Los Alamos radiative opacity in cm^2 g^{-1} (opacity), the mesh number (mesh). For the atmosphere and the subatmosphere μ, opac., G_{ad}, G_{con}, log G indicate respectively the molecular weight, the value of the Los Alamos radiative opacity in cm^2 g^{-1}, the adiabatic gradient, the superadiabatic gradient, the logarithm of the surface gravity in cm s^{-2} ($Y = 0.295$, $Z = 0.0190$, $\alpha = 1.87$, $L = 3.83\,10^{33}$ erg s^{-1}, $R = 6.96\,10^{10}$ cm, $T_c = 1.57\,10^7$ K)

interior

M/M_t	R/R_t	log P	log T	log ρ	L/L_{sup}	ε_{nuc}	pp	^{7}Be	^{8}B	G_{rad}	H	Opacity	Mesh
0.0000001	0.00068	17.3674	7.1964	2.1775	9.29512D−07	1.734D+01	2.152D+32	9.142D+31	3.23D+29	3.375D−01	3.34D−01	1.29D+00	1
0.0000077	0.00415	17.3669	7.1963	2.1768	6.96207D−05	1.731D+01	5.381D+33	2.276D+33	8.02D+30	3.374D−01	3.35D−01	1.29D+00	5
0.0004127	0.01567	17.3601	7.1940	2.1693	3.64753D−03	1.683D+01	2.151D+35	8.625D+34	2.87D+32	3.356D−01	3.41D−01	1.30D+00	10
0.0046436	0.03581	17.3311	7.1844	2.1365	3.84828D−02	1.536D+01	1.076D+36	3.453D+35	9.00D+32	3.308D−01	3.70D−01	1.34D+00	15
0.0098032	0.04654	17.3080	7.1767	2.1107	7.83957D−02	1.445D+01	1.069D+36	2.872D+35	6.14D+32	3.319D−01	3.94D−01	1.37D+00	20
0.0185745	0.05851	17.2767	7.1663	2.0777	1.40602D−01	1.305D+01	2.064D+36	4.334D+35	6.98D+32	3.309D−01	4.21D−01	1.41D+00	25
0.0278617	0.06795	17.2484	7.1570	2.0484	2.01069D−01	1.201D+01	1.982D+36	3.340D+35	4.14D+32	3.303D−01	4.46D−01	1.44D+00	30
0.0381808	0.07653	17.2202	7.1477	2.0204	2.62727D−01	1.102D+01	1.880D+36	2.550D+35	2.42D+32	3.295D−01	4.68D−01	1.48D+00	35
0.0485000	0.08392	17.1943	7.1392	1.9954	3.19399D−01	1.014D+01	1.774D+36	1.974D+35	1.45D+32	3.285D−01	4.87D−01	1.51D+00	40
0.0588191	0.09053	17.1699	7.1312	1.9725	3.71653D−01	9.365D+00	1.669D+36	1.544D+35	8.94D+31	3.274D−01	5.04D−01	1.54D+00	45
0.0691383	0.09658	17.1467	7.1236	1.9513	4.19936D−01	8.660D+00	1.567D+36	1.218D+35	5.59D+31	3.261D−01	5.19D−01	1.57D+00	50
0.0887447	0.10694	17.1049	7.1100	1.9147	5.00938D−01	7.393D+00	2.757D+36	1.569D+35	4.71D+31	3.227D−01	5.41D−01	1.63D+00	55
0.1093829	0.11677	17.0632	7.0966	1.8789	5.74544D−01	6.364D+00	2.408D+36	1.017D+35	1.99D+31	3.189D−01	5.62D−01	1.68D+00	60
0.1300213	0.12582	17.0231	7.0839	1.8455	6.37925D−01	5.482D+00	2.096D+36	6.696D+34	8.68D+30	3.151D−01	5.80D−01	1.74D+00	65
0.1506596	0.13430	16.9841	7.0717	1.8137	6.92510D−01	4.718D+00	1.817D+36	4.461D+34	3.86D+30	3.107D−01	5.95D−01	1.79D+00	70
0.1712979	0.14237	16.9459	7.0600	1.7827	7.39440D−01	4.054D+00	1.569D+36	2.999D+34	1.75D+30	3.060D−01	6.08D−01	1.84D+00	75
0.1919362	0.15010	16.9083	7.0485	1.7526	7.79765D−01	3.484D+00	1.352D+36	2.033D+34	8.01D+29	3.011D−01	6.19D−01	1.88D+00	80
0.2141223	0.15815	16.8682	7.0365	1.7211	8.16739D−01	2.945D+00	1.436D+36	1.678D+34	4.37D+29	2.958D−01	6.29D−01	1.94D+00	85
0.2394043	0.16704	16.8227	7.0232	1.6855	8.52013D−01	2.448D+00	9.519D+35	8.496D+33	1.38D+29	2.895D−01	6.39D−01	2.00D+00	90
0.2708777	0.17782	16.7660	7.0071	1.6419	8.87172D−01	1.914D+00	9.368D+35	6.005D+33	5.49D+28	2.815D−01	6.49D−01	2.07D+00	95
0.2966755	0.18650	16.7193	6.9941	1.6060	9.10385D−01	1.562D+00	7.669D+35	3.788D+33	2.16D+28	2.750D−01	6.55D−01	2.13D+00	100
0.3289229	0.19724	16.6602	6.9780	1.5607	9.33279D−01	1.193D+00	8.902D+35	3.169D+33	1.00D+28	2.674D−01	6.62D−01	2.22D+00	105
0.3676197	0.21008	16.5878	6.9590	1.5056	9.53849D−01	8.702D−01	6.495D+35	1.593D+33	2.47D+27	2.584D−01	6.68D−01	2.32D+00	110
0.4063165	0.22299	16.5133	6.9401	1.4491	9.68794D−01	6.298D−01	4.688D+35	7.958D+32	6.00D+26	2.502D−01	6.73D−01	2.44D+00	115
0.4450133	0.23612	16.4360	6.9210	1.3899	9.79555D−01	4.512D−01	3.336D+35	3.928D+32	1.42D+26	2.424D−01	6.76D−01	2.57D+00	120
0.4837101	0.24960	16.3553	6.9018	1.3278	9.87230D−01	3.210D−01	2.336D+35	1.913D+32	3.22D+25	2.350D−01	6.79D−01	2.71D+00	125
0.5133777	0.26027	16.2905	6.8867	1.2780	9.91598D−01	2.484D−01	1.171D+35	7.322D+31	6.75D+24	2.297D−01	6.80D−01	2.83D+00	130
0.5494947	0.27377	16.2078	6.8680	1.2142	9.95401D−01	1.615D−01	8.132D+34	3.273D+31	1.41D+24	2.236D−01	6.81D−01	2.99D+00	135
0.5752926	0.28383	16.1457	6.8542	1.1661	9.97142D−01	1.021D−01	6.186D+34	1.518D+31	3.70D+23	2.195D−01	6.82D−01	3.11D+00	140
0.6010904	0.29431	16.0806	6.8401	1.1153	9.98202D−01	6.161D−02	4.646D+34	5.862D+30	7.90D+22	2.156D−01	6.83D−01	3.25D+00	145
0.6268883	0.30531	16.0121	6.8254	1.0617	9.98851D−01	3.945D−02	3.438D+34	1.970D+30	1.43D+22	2.118D−01	6.84D−01	3.41D+00	150
0.6526862	0.31690	15.9396	6.8102	1.0044	9.99275D−01	2.686D−02	2.498D+34	5.973D+29	2.26D+21	2.082D−01	6.84D−01	3.58D+00	155
0.6784841	0.32923	15.8627	6.7943	.9431	9.99564D−01	1.868D−02	1.778D+34	1.656D+29	3.15D+20	2.048D−01	6.85D−01	3.78D+00	160
0.7042819	0.34244	15.7805	6.7776	.8773	9.99759D−01	1.289D−02	1.236D+34	4.193D+28	3.82D+19	2.013D−01	6.85D−01	3.99D+00	165
0.7300798	0.35671	15.6921	6.7600	.8065	9.99889D−01	8.699D−03	8.356D+33	9.580D+27	3.97D+18	1.981D−01	6.85D−01	4.24D+00	170

Table A5 (continued)

M/M_t	R/R_t	log P	log T	log ρ	L/L_{sup}	ε_{nuc}	pp	^{7}Be	^{8}B	G_{rad}	H	Opacity	Mesh
0.7558777	0.37226	15.5963	6.7412	.7296	9.99970D−01	5.687D−03	5.466D+33	1.936D+27	3.42D+17	1.950D−01	6.86D−01	4.53D+00	175
0.7816755	0.38942	15.4915	6.7209	.6454	1.00002D+00	3.571D−03	3.432D+33	3.361D+26	2.33D+16	1.923D−01	6.86D−01	4.88D+00	180
0.8074734	0.40860	15.3757	6.6988	.5516	1.00004D+00	2.128D−03	2.046D+33	4.812D+25	1.18D+15	1.898D−01	6.86D−01	5.30D+00	185
0.8332713	0.43042	15.2457	6.6742	.4462	1.00005D+00	1.188D−03	1.141D+33	5.376D+24	4.08D+13	1.878D−01	6.86D−01	5.82D+00	190
0.8590691	0.45578	15.0974	6.6465	.3258	1.00005D+00	6.065D−04	5.829D+32	4.297D+23	8.37D+11	1.868D−01	6.86D−01	6.50D+00	195
0.8848671	0.48611	14.9239	6.6140	.1849	1.00004D+00	2.731D−04	2.625D+32	2.121D+22	8.10D+09	1.878D−01	6.86D−01	7.45D+00	200
0.9106649	0.52385	14.7137	6.5742	.0146	1.00003D+00	1.015D−04	9.752D+31	4.946D+20	2.41D+07	1.910D−01	6.86D−01	8.76D+00	205
0.9364628	0.57371	14.4448	6.5219	−0.2019	1.00002D+00	2.727D−05	2.621D+31	3.207D+18	9.36D+03	1.988D−01	6.86D−01	1.08D+01	210
0.9532314	0.61720	14.2154	6.4751	−0.3844	1.00001D+00	8.379D−06	4.027D+30	1.473D+16	3.12D+00	2.118D−01	6.86D−01	1.29D+01	215
0.9648404	0.65621	14.0131	6.4303	−0.5417	1.00000D+00	2.739D−06	1.053D+30	1.302D+14	2.02D−03	2.338D−01	6.86D−01	1.52D+01	220

Atmosphere and subatmosphere

M/M_t	log P	log T	log ρ	R/R_t	μ	Opac.	G_{rad}	G_{ad}	G_{con}	log G	Mesh
0.9700	13.904	6.405	−.625	0.6769	0.623	1.218	2.489E−01	.397	.000	4.763	238
0.9925	13.077	6.105	−1.151	0.8180	0.623	1.715	1.809E+00	.398	.398	4.609	217
0.9996	11.587	5.510	−2.033	0.9448	0.646	2.836	1.832E+02	.396	.396	4.487	181
1.0000	10.097	4.945	−2.932	0.9827	0.685	4.735	8.537E+04	.357	.357	4.453	145
1.0000	8.607	4.515	−3.928	0.9935	0.796	4.940	2.335E+05	.213	.213	4.443	109
1.0000	7.117	4.256	−5.066	0.9976	0.988	3.828	6.300E+03	.138	.143	4.440	73
1.0000	5.626	4.036	−6.231	0.9996	1.254	2.267	4.278E+01	.139	.215	4.438	37
1.0000	5.033	3.784	−6.543	1.000	1.343	−.371	2.546E−01	.383	.000	4.438	1

References

Abazov et al., 1991, Phys. Rev. Lett. 24, 3332

Anders E., Grevesse N., 1989, Geochim. Cosmochim. Acta 53, 197

Arpesella C., Bellini G., Raghavan R., et al., 1992, Borexino at Gran Sasso (the Borexino proposal preprint INFN Milano)

Arpesella C., et al., 1991, preprint LNGS-91/18

Bahcall J.N., 1989, Neutrino Astrophysics, Cambridge University Press, Cambridge

Bahcall J.N., Pinsonneault M.H., 1992, preprint IASSNS-AST 92/10

Bahcall J.N., Ulrich R.K., 1988, Rev. Mod. Phys. 60, 297

Bahcall J.N., Cabibbo A., Yahill A., 1972, Phys. Rev. Lett. 28, 316

Bahcall J.N., Cleveland B.T., Davis R., Rowley J.K, 1985, ApJ 292, L79

Berezhiani Z.G., Vysotskii M.I., 1987, Phys. Lett. B 199, 281

Bethe H.A., Bahcall J.N., 1991, Phys. Rev. D 44, 2962

Castellani V., Chieffi A., Pulone L., 1991, ApJS 76, 911

Castellani V., Chieffi A., Straniero O., 1992, ApJS 78, 517

Caughlan G.R., Fowler W.A., 1988, Atomic Data Nucl. Data Tables, 40, 283

Chieffi A., Straniero O., 1989, ApJS 71, 47

Cox A.N., Tabor J.E., 1976, ApJS 31, 271

Davis R., et al. 1990, in: Proc. Int. Conf. Neutrino 90, Geneva

DeWitt H., Graboske H., Cooper M., 1973, ApJ 181, 439

Fowler W.A., 1972, Nat 238, 24

Graboske H., DeWitt H., Grossman A., Cooper M., 1973, ApJ 181, 457

Grevesse N., 1984, Phys. Scripta T8, 49

Gribov V., Pontecorvo B., 1969, Phys. Lett. B28, 493

Hirata K., et al., 1990, Phys. Rev. Lett. 65, 1297

Hirata K., et al., 1991, Phys. Rev. Lett. 66, 9

Huebner W.F., Merts A.L., Magee N.H., Argo M.F., 1977, Los Alamos Sci. Lab. Report (LA-6760-M)

Iglesias C.P., Rogers F.J., 1991, ApJ 371, 408

Krauss A., Becker H.W., Trautvetter H.P., Rolfs C., 1987, Nucl. Phys. A 467, 273

Mikheyev S.P., Smirnov A. Yu., 1986a, Sov. J. Nucl. Phys. 42, 913

Mikheyev S.P., Smirnov A. Yu., 1986b, Sov. Phys.- JETP 64, 4

Parker P.D. 1986, in: Sturrock P.A. (ed.) Physics of the Sun, Vol. I, Reidel, New York. p. 15

Pontecorvo B., 1968, Sov. Phys. - JETP 26, 984

Raghavan R.S., 1990 in: Phua K.K., Yamaguchi Y. (eds.) Proc. 25th Int. Conf. High Energy Physics, Vol. 1. Singapore, World Scientific, Singapore, p. 482.

Ratcliff S.J., 1987, ApJ 318, 196

Rolfs C., Rodney W., 1988, Cauldrons in the Cosmos. University of Chicago Press, Chicago

Ross J.E., Aller L.H., 1976, Sci 191, 1223

Sackmann I.J., Boothroyd A.I., Fowler W.A., 1990, ApJ 360, 727

Straniero O., 1988, A&AS 76, 157

Turck-Chièze S., Lopez I., 1992, ApJ (submitted); Proc. XIIth Moriond Workshop, January 1992, ed. Frontieres (to be published)

Turck-Chièze S., Cahen S., Cassé M., Doom C., 1988, ApJ 335, 415

Voloshin M.B., Vysotskii M.I., Okun L.B., 1986a, Sov. J. Nucl. Phys. 42, 913

Voloshin M.B., Vysotskii M.I., Okun L.B., 1986b, Sov. Phys. -JETP 64, 446

Wolfenstein L., 1979, Phys. Rev. D 20, 2634